Disrupting galectin-1 interactions with N-glycans suppresses hypoxia-driven angiogenesis and tumorigenesis in Kaposi's sarcoma

Diego O. Croci,[1,2] Mariana Salatino,[1,2] Natalia Rubinstein,[2] Juan P. Cerliani,[1] Lucas E. Cavallin,[3] Howard J. Leung,[3] Jing Ouyang,[4] Juan M. Ilarregui,[1,2] Marta A. Toscano,[1,2] Carolina I. Domaica,[1,2] María C. Croci,[5] Margaret A. Shipp,[4] Enrique A. Mesri,[3] Adriana Albini,[6] and Gabriel A. Rabinovich[1,2,7]

[1]Laboratorio de Inmunopatología, Instituto de Biología y Medicina Experimental, Consejo Nacional de Investigaciones Científicas y Técnicas, 1428 Buenos Aires, Argentina
[2]División Inmunogenética, Hospital de Clínicas "José de San Martín," Universidad de Buenos Aires, 1120 Buenos Aires, Argentina
[3]Viral Oncology Program, Sylvester Comprehensive Cancer Center, Miami Center for AIDS Research, Department of Microbiology and Immunology, Miller School of Medicine, University of Miami, Miami, FL 33136
[4]Department of Medical Oncology, Dana Farber Cancer Institute, Boston, MA 02215
[5]Laboratorio de Patología, Facultad de Ciencias Médicas, Universidad Nacional del Comahue, 8324 Cipolletti, Argentina
[6]Polo Scientifico e Tecnologico, Istituto di Ricovero e Cura a Carattere Scientifico MultiMedica, 20138 Milano, Italy
[7]Departamento de Química Biológica, Facultad de Ciencias Exactas y Naturales, Universidad de Buenos Aires, 1428 Buenos Aires, Argentina

Kaposi's sarcoma (KS), a multifocal vascular neoplasm linked to human herpesvirus-8 (HHV-8/KS-associated herpesvirus [KSHV]) infection, is the most common AIDS-associated malignancy. Clinical management of KS has proven to be challenging because of its prevalence in immunosuppressed patients and its unique vascular and inflammatory nature that is sustained by viral and host-derived paracrine-acting factors primarily released under hypoxic conditions. We show that interactions between the regulatory lectin galectin-1 (Gal-1) and specific target N-glycans link tumor hypoxia to neovascularization as part of the pathogenesis of KS. Expression of Gal-1 is found to be a hallmark of human KS but not other vascular pathologies and is directly induced by both KSHV and hypoxia. Interestingly, hypoxia induced Gal-1 through mechanisms that are independent of hypoxia-inducible factor (HIF) 1α and HIF-2α but involved reactive oxygen species–dependent activation of the transcription factor nuclear factor κB. Targeted disruption of Gal-1–N-glycan interactions eliminated hypoxia-driven angiogenesis and suppressed tumorigenesis in vivo. Therapeutic administration of a Gal-1–specific neutralizing mAb attenuated abnormal angiogenesis and promoted tumor regression in mice bearing established KS tumors. Given the active search for HIF-independent mechanisms that serve to couple tumor hypoxia to pathological angiogenesis, our findings provide novel opportunities not only for treating KS patients but also for understanding and managing a variety of solid tumors.

Kaposi's sarcoma (KS) is a multifocal vascular neoplasm strictly associated with infection by the KS-associated herpesvirus (KSHV or HHV8) that occurs in several clinical-epidemiological settings, typically in the context of immunodeficiency (Mesri et al., 2010). This enigmatic tumor, which has emerged as a model of pathological angiogenesis, is the most common

CORRESPONDENCE
Gabriel A. Rabinovich:
gabyrabi@gmail.com

Abbreviations used: ANGPTL4, angiopoietin-like 4; C/EBPα, CCAAT/enhanced binding protein α; C2GnT-1, core-2 β1-6-*N*-acetylglucosaminyltransferase-1; EC, endothelial cell; EdU, 5-ethynyl-2′-deoxyuridine; Gal-1, galectin-1; GnT5, *N*-acetylglucosaminyltransferase 5; HIF, hypoxia-inducible factor; HUVEC, human umbilical vein EC; KS, Kaposi's sarcoma; KSHV, KS-associated herpesvirus; LacNAc, galactose-β1-4-*N*-acetylglucosamine; NAC, *N*-acetylcysteine; ROS, reactive oxygen species; SFCM, serum-free conditioned medium; shRNA, short hairpin RNA; VEGF, vascular endothelial growth factor; vGPCR, viral G protein–coupled receptor.

M. Salatino and N. Rubinstein contributed equally to this paper.
N. Rubinstein's present address is Instituto de Fisiología, Biología Molecular y Neurociencias, Facultad de Ciencias Exactas y Naturales, Universidad de Buenos Aires, 1428 Buenos Aires, Argentina.

The Rockefeller University Press $30.00
J. Exp. Med. 2012 Vol. 209 No. 11 1985-2000
www.jem.org/cgi/doi/10.1084/jem.20111665

The Journal of Experimental Medicine

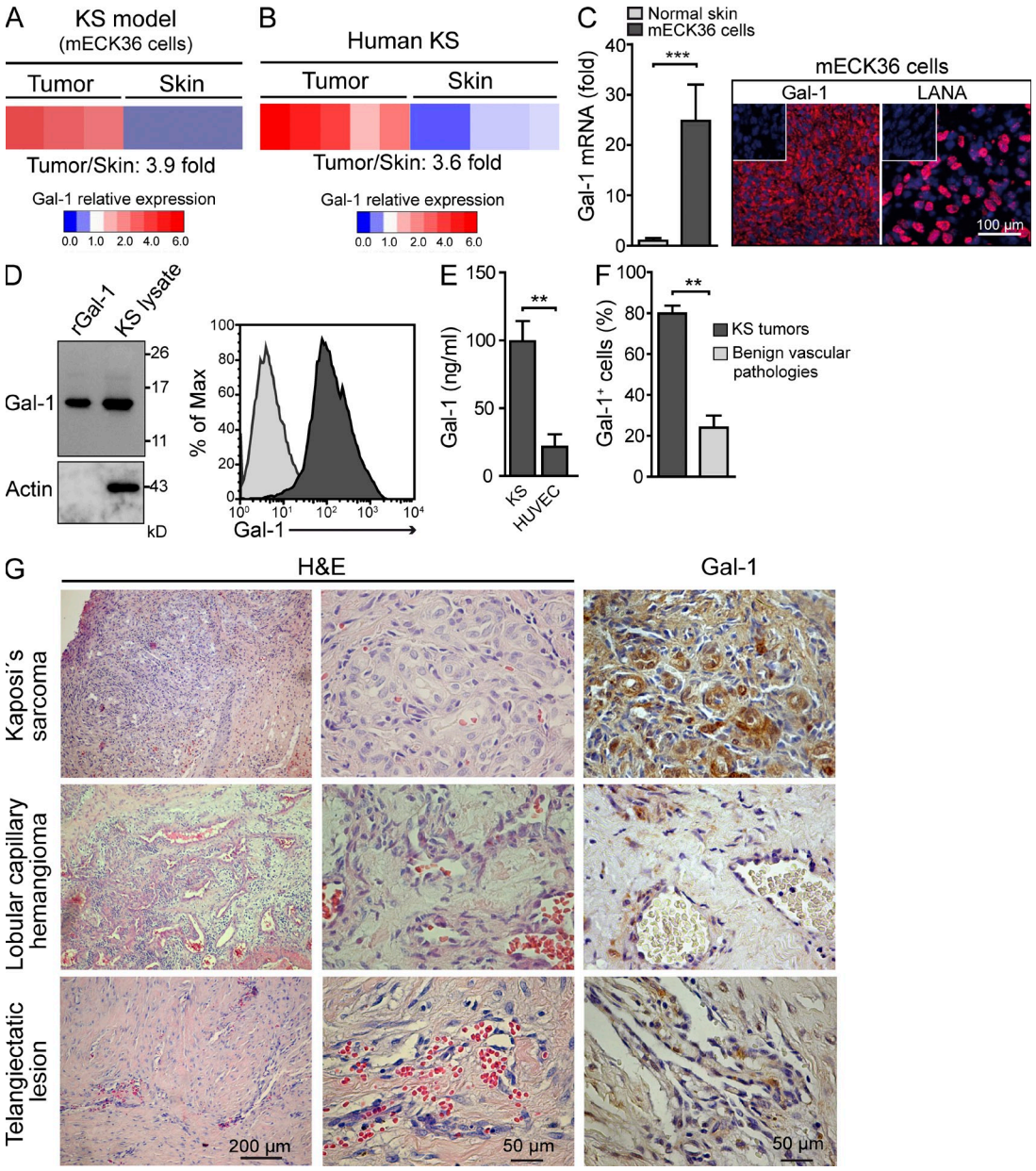

Figure 1. Gal-1 expression is a hallmark of KS. (A and B) Gal-1 transcript profile of mouse mECK36 KS tumors and human AIDS-KS compared with normal skin (Array data were obtained from Mutlu et al., 2007 and from Wang et al., 2004). (C) Left, qRT-PCR analysis of Gal-1 mRNA in mECK36 KS tumors and normal skin. Results are the mean ± SEM of three independent experiments. Right, confocal microscopy of mECK36 tumors stained for Gal-1 and LANA. Data are representative of three independent experiments. (D) Left, immunoblot of Gal-1 in KS-Imm cells. Right, flow cytometry of Gal-1 in permeabilized KS cells. Data are representative of six experiments. (E) ELISA of Gal-1 secretion by KS cells and HUVEC. Data are the mean ± SEM of three independent experiments. (F and G) Immunohistochemical analysis of human benign vascular lesions (n = 26) and primary KS tumors (n = 15) stained with anti-Gal-1 polyclonal Ab or with H&E. Data are the mean ± SEM (F) .Representative micrographs are shown (G). (C, E, and F) **, $P < 0.01$; ***, $P < 0.001$.

malignancy in HIV-infected individuals and is a leading cause of morbidity and mortality in AIDS (Casper, 2011).

Although the pathogenesis of KS is not completely understood, recent evidence suggests that KSHV-encoded lytic genes induce the release of host and viral growth factors, including vascular endothelial growth factor (VEGF), angiopoietin-like 4 (ANGPTL4), and IL-8, which may act together in a paracrine manner to drive proliferation, angiogenesis, and inflammation (Cesarman et al., 2000; Montaner et al., 2006; Sun et al., 2006; Ma et al., 2010). The concerted action of these paracrine-acting factors, mostly released under hypoxic conditions, may contribute to the unique angioproliferative nature of these tumors.

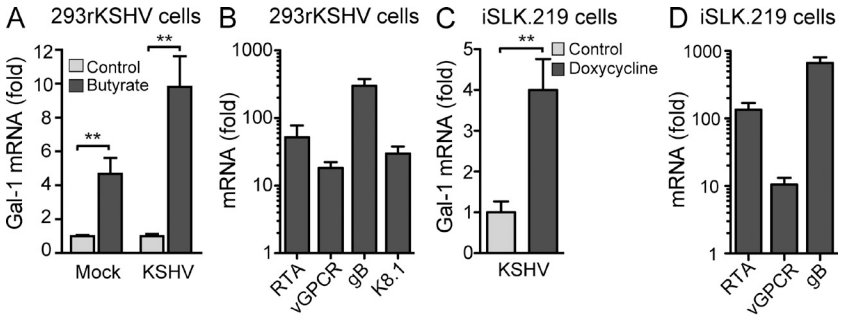

Figure 2. KSHV controls Gal-1 expression. (A) qRT-PCR analysis of Gal-1 mRNA in uninfected 293 and 293rKSHV.219 cells upon stimulation with 3 mM sodium butyrate to induce lytic gene expression. Data indicate fold increase of mRNA as measured by triplicates of two independent experiments. (B) KSHV lytic gene expression (RTA, vGPCR, gB, K8.1) in 293rKSHV cells upon stimulation with sodium butyrate for 24 h. Data indicate fold increase of mRNA as measured by triplicates of two independent experiments. (C) qRT-PCR analysis of Gal-1 mRNA in iSLK.219 cells upon stimulation with doxycycline to induce RTA-driven lytic gene expression. Data indicate fold increase of mRNA as measured by triplicates of two independent experiments. (D) KSHV lytic gene expression (RTA, vGPCR, gB) in iSLK.219 cells upon stimulation with doxycycline. Data indicate fold increase of mRNA as measured by triplicates of two independent experiments. (A–D) Error bars represent SEM. (A and C) **, $P < 0.01$.

Despite a decline in its incidence with the widespread use of HAART (highly active antiretroviral therapy), KS progresses in most patients within 6 mo of treatment and often requires additional therapy. Unfortunately, current treatment options are only palliative and include chemotherapeutic drugs, which are themselves associated with immunosuppression and cumulative toxicity (Mesri et al., 2010). Recent findings have identified novel molecular pathways of viral-induced KS signaling, survival, and angiogenesis which could be targeted by drugs; these include KHSV-dependent activation of PI3K (phosphatidylinositol 3-kinase)/Akt/mTOR, small GTPase Rac1, and NF-κB (Montaner et al., 2004; Chaisuparat et al., 2008; Martin et al., 2008, 2011). However, the molecular pathways coupling viral infection and tumor hypoxia to angiogenesis are poorly understood.

Recent efforts toward deciphering the information encoded by the glycome—the complete repertoire of glycans that cells synthesize under specific conditions of time, space, and environment—have revealed novel opportunities for differential diagnosis, prognosis, and therapeutic intervention (Paulson et al., 2006). The responsibility for decoding this information is assigned to endogenous glycan-binding proteins or lectins, which typically establish multivalent interactions with cell surface glycans to control immune cell signaling, inflammation, and neovascularization (Markowska et al., 2010; Rabinovich and Croci, 2012). Galectin-1 (Gal-1), a member of a highly conserved family of animal lectins, is released by a variety of tumors where it contributes to malignant transformation and metastasis (Paz et al., 2001; Liu and Rabinovich, 2005). Previous studies identified an essential role for this lectin in controlling inflammation (Rabinovich et al., 1999; Rabinovich and Croci, 2012) and promoting tumor-immune escape (Rubinstein et al., 2004; Juszczynski et al., 2007; Banh et al., 2011; Kuo et al., 2011; Cedeno-Laurent et al., 2012; Tang et al., 2012). The mechanisms underlying these effects involve glycosylation-dependent control of T helper cell survival (Toscano et al., 2007), modulation of T cell trafficking (Norling et al., 2008), and induction of tolerogenic dendritic cells (Ilarregui et al., 2009). Interestingly, Gal-1 is also part of the hypoxia-regulated transcriptome (Le et al., 2005) and controls endothelial cell (EC) signaling (Hsieh et al., 2008; Thijssen et al., 2010).

Given the prevalence of KS in immunosuppressed individuals and its unique vascular nature, we hypothesized that interactions between Gal-1 and specific N-glycans may contribute to the pathogenesis of KS. In this study, we demonstrate a novel role for Gal-1–N-glycan interactions in coupling tumor hypoxia to pathological angiogenesis in KS. Moreover, we validate the in vivo therapeutic efficacy of a blocking anti-Gal1 mAb, which promotes tumor regression and attenuates abnormal angiogenesis, thus providing novel opportunities for treating not only KS but also a variety of tumors.

RESULTS

Gal-1 expression is a hallmark of KS

To study the contribution of Gal-1 to the pathogenesis of KS, we first examined the relative expression profile of this lectin in the mouse mECK36 KS-like tumor and human AIDS-KS transcriptomes. mECK36 is a cell model of KSHV-induced KS generated by transfection of a KSHV bacterial artificial chromosome (KSHVBac36) into ECs which then form spindle cell sarcomas reminiscent of KS when injected into nude mice (Mutlu et al., 2007). We found that Gal-1 transcripts were part of both the mouse KS-like and the AIDS-KS signature because they were overexpressed ∼3.9-fold in mECK36 tumors and ∼3.6-fold in AIDS-KS lesions (Fig. 1, A and B) when compared with skin, the control tissue against which the KS molecular signature was originally defined (Wang et al., 2004). Overexpression was confirmed by quantitative (q) RT-PCR and immunofluorescence of KSHV-infected mECK36 LANA$^+$ tumors (Fig. 1 C). This lectin was mainly localized in the intracellular compartment of permeabilized human KS cells and secreted to the extracellular medium of these cells (Fig. 1, D and E), suggesting that Gal-1 may represent an alternative paracrine factor that contributes to the proangiogenic phenotype induced by KSHV. Of note, the amounts of Gal-1 secreted by KS spindle cells were substantially higher than those produced by nontransformed human umbilical vein ECs (HUVECs; Fig. 1 E).

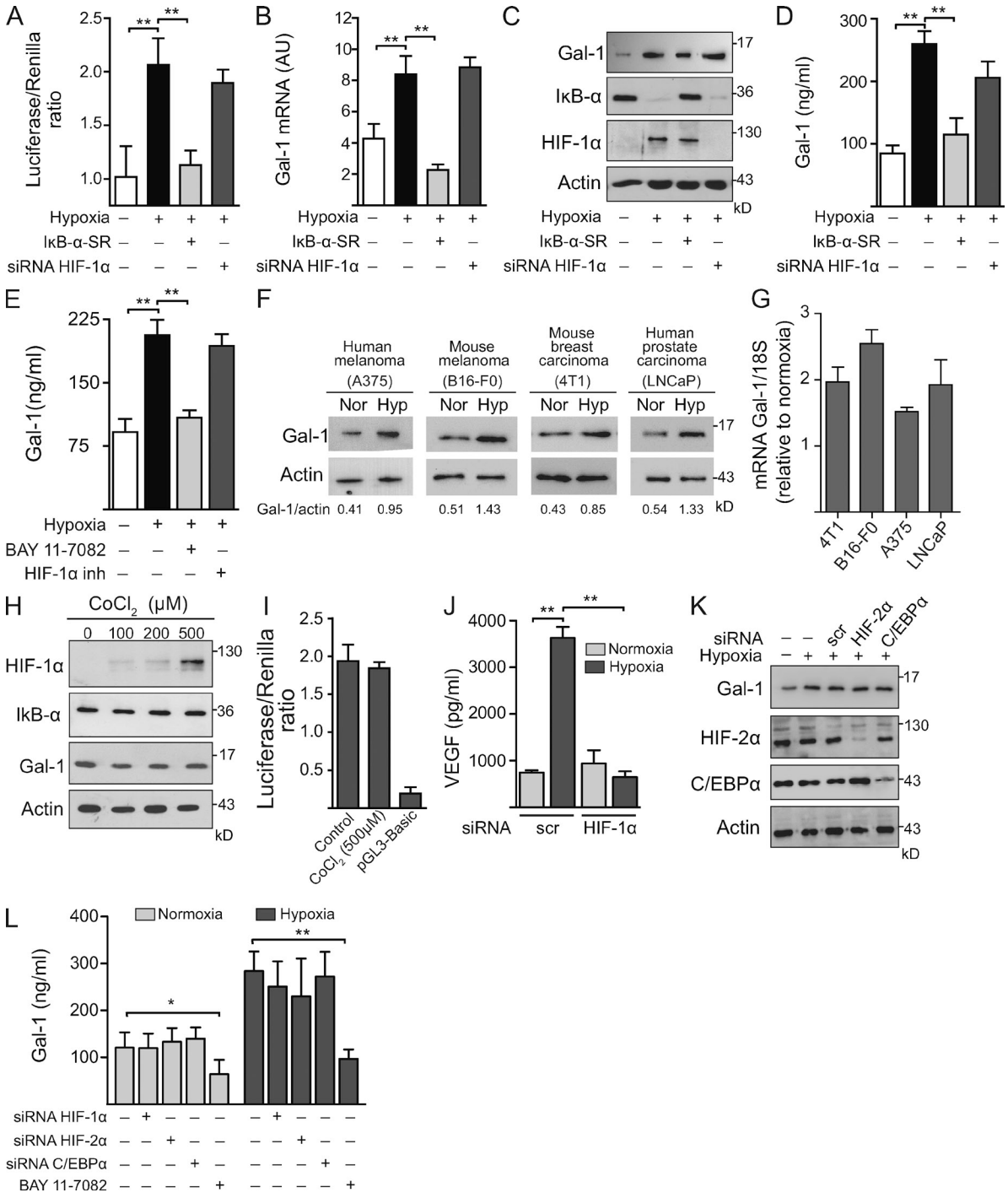

Figure 3. Hypoxia controls Gal-1 expression in KS through HIF-independent, NF-κB–dependent mechanisms. (A–D) Expression of Gal-1 in KS cells transfected with or without HIF-1α siRNA or a super-repressor form of IκB-α (IκB-α-SR) and incubated under hypoxia or normoxia. (A) Promoter activity. (B) qRT-PCR of Gal-1 mRNA relative to RN18S1. AU, arbitrary units. Data are the mean ± SEM of five (A) or three (B) independent experiments. (C) Immunoblot of Gal-1, IκB-α, HIF-1α, and actin. Data are representative of four independent experiments. (D) ELISA of Gal-1 secretion. Data are the mean ± SEM of three independent experiments. (E) ELISA of Gal-1 secretion by KS cells cultured under hypoxic or normoxic conditions in the presence or absence of HIF-1α or NF-κB inhibitors. Data are the mean ± SEM of three independent experiments. (F and G) Immunoblot (F) and qRT-PCR (G) of Gal-1 expression induced by hypoxia (Hyp) in human and mouse melanoma (A375 and B16-F0), mouse breast carcinoma (4T1), and human prostate carcinoma (LNCaP) cell lines. Data are representative (F) or are the mean ± SEM (G) of three independent experiments. (H) Western blot of HIF-1α, IκB-α, Gal-1, and actin upon treatment of KS cells with $CoCl_2$ (chemical activator of HIF-1α). Data are representative of four experiments. (I) Gal-1 promoter activity upon treatment of KS cells with $CoCl_2$. Modulation of pGL3-Gal-1–Luciferase activity relative to Renilla expression is shown. Data are the mean ± SEM of three independent experiments. (J) ELISA of VEGF secretion

KS lesions, irrespective of their epidemiological forms, are similarly comprised of KSHV-infected spindle cells, vessels, and inflammatory infiltrates (Ganem, 2010). To determine the clinicopathologic relevance of our findings, we further examined a collection of biopsies from KS patients, including HIV$^-$ classical KS and AIDS-KS, together with a series of benign vascular pathologies. Remarkably, Gal-1 was selectively expressed in KS lesions associated with vascular channels, showing robust cytoplasmic and weak membrane staining in spindle cells. In contrast, Gal-1 was barely detected in benign vascular lesions, including lobular capillary hemangioma and telangiectatic lesions, in which only diffuse staining of inflammatory infiltrates was detected (Fig. 1, F and G). Collectively, these data suggest a role for Gal-1 in KS pathogenesis and its potential use as a diagnostic biomarker capable of delineating highly tumorigenic human KS from benign vascular lesions with shared morphological and molecular features.

KSHV controls Gal-1 expression

To examine the ability of KSHV infection to regulate Gal-1 expression directly in human cells, we used the HEK293 cell line harboring latent recombinant rKSHV.219 (HEK-293rKSHV.219) that expresses GFP during latent and lytic replication and RFP during lytic replication (Vieira and O'Hearn, 2004). When HEK293rKSHV.219 cells were treated with sodium butyrate to induce viral lytic replication, we found a twofold up-regulation of Gal-1 along with the expression of lytic genes (Fig. 2, A and B), suggesting a role of Gal-1 in KSHV sarcomagenesis. As butyrate treatment affects Gal-1 expression, we next used a more specific system of viral lytic replication comprising inducible SLK (iSLK), a KS spindle cell of endothelial lineage infected with rKSHV.219 in which lytic replication is induced by a Tet-inducible RTA (Myoung and Ganem, 2011). We found that Tet induction of RTA-driven lytic replication led to a fourfold increase in Gal-1 expression (Fig. 2, C and D). These results suggest that Gal-1 may be part of the angioproliferative program that is up-regulated in KS spindle cells during KSHV lytic replication and participates in KS pathogenesis.

Hypoxia controls Gal-1 expression in KS cells through mechanisms involving reactive oxygen species (ROS)–dependent NF-κB activation

The concerted action of hypoxia-regulated pathways allows tumor cells to sprout new vessels, co-opt host vessels, and/or recruit angiocompetent bone marrow–derived cells to generate functionally abnormal tumor vasculatures (Fraisl et al., 2009; Chung and Ferrara, 2011). This effect is particularly relevant in the context of KS given the direct effects of hypoxia on KSHV lytic replication, the ability of KSHV to increase the expression of hypoxia-inducible factors (HIFs), and the angioproliferative nature of this tumor (Haque et al., 2003; Mesri et al., 2010).

To investigate whether lectin–glycan interactions link tumor hypoxia to sprouting angiogenesis in KS, we first examined the regulated expression of tumor-derived Gal-1 under hypoxic or normoxic conditions in AIDS-KS spindle (KS-Imm) cells (Albini et al., 2001). Hypoxia induced considerable up-regulation of Gal-1 in KS cells as shown by *LGALS1* promoter activity, Gal-1 mRNA, and Gal-1 protein expression and secretion, as compared with KS cells grown under normoxic conditions (Fig. 3, A–E). Hypoxia-induced Gal-1 expression was also evident at both mRNA and protein levels and in human and mouse melanoma (A375 and B16-F0), mouse breast carcinoma (4T1), and human prostate carcinoma (LNCaP) cell lines (Fig. 3, F and G), suggesting broad regulation of endogenous Gal-1 at the transcriptional level in tumors of either mesenchymal or epithelial origin.

Given the relevance of HIF-1α in hypoxia-driven angiogenesis, we then examined whether this master transcription factor may control hypoxia-induced Gal-1 expression in KS cells. Remarkably, hypoxia induced up-regulation of Gal-1 in either KS cells transfected with HIF-1α siRNA (Fig. 3, A–D) or in KS cells incubated with a specific HIF-1α inhibitor (Fig. 3 E). Consistent with these observations, chemical activation of HIF-1α had no effect on Gal-1 expression (Fig. 3, H and I). However, knocking down HIF-1α efficiently prevented hypoxia-induced secretion of VEGF (Fig. 3 J), a well established target of this transcriptional factor (Fraisl et al., 2009). Because HIF-2α may compensate for HIF-1α in certain systems and these related transcription factors can induce distinct gene expression profiles (Keith et al., 2012), we then examined whether HIF-2α may control Gal-1 expression in KS cells. Notably, siRNA-mediated silencing of HIF-2α did not prevent hypoxia-induced Gal-1 expression and secretion (Fig. 3, K and L), suggesting that HIF-independent mechanisms operate, at least in KS cells, to control hypoxia-driven Gal-1 expression. As Gal-1 has been recently identified as a direct transcriptional target of CCAAT/enhanced binding protein α (C/EBPα) in acute myeloid leukemic cells (Zhao et al., 2011) and this transcription factor plays an important role during KS development (Wu et al., 2002), we then analyzed whether C/EBPα contributes to hypoxia-driven Gal-1 expression in KS. However, knocking down C/EBPα did not alter Gal-1 expression or secretion by KS cells exposed to either hypoxic or normoxic conditions (Fig. 3, K and L).

by KS cells transfected with HIF-1α or scr siRNA cultured under hypoxic or normoxic conditions. Data are the mean ± SEM of three independent experiments. (K) Immunoblot of Gal-1, HIF-2α, c/EBPα, and actin in KS cells transfected with or without siRNA for HIF-2α, C/EBPα, or scrambled (scr) and incubated under hypoxia or normoxia. Data are representative of three independent experiments. (L) ELISA of Gal-1 secretion by KS cells transfected with or without siRNA for HIF-1α, HIF-2α, or C/EBPα or incubated with an NF-κB inhibitor (BAY 11–7082; 1 μM) and cultured under hypoxic or normoxic conditions. Data are the mean ± SEM of three independent experiments. (A, B, D, E, J, and L) *, $P < 0.05$; **, $P < 0.01$.

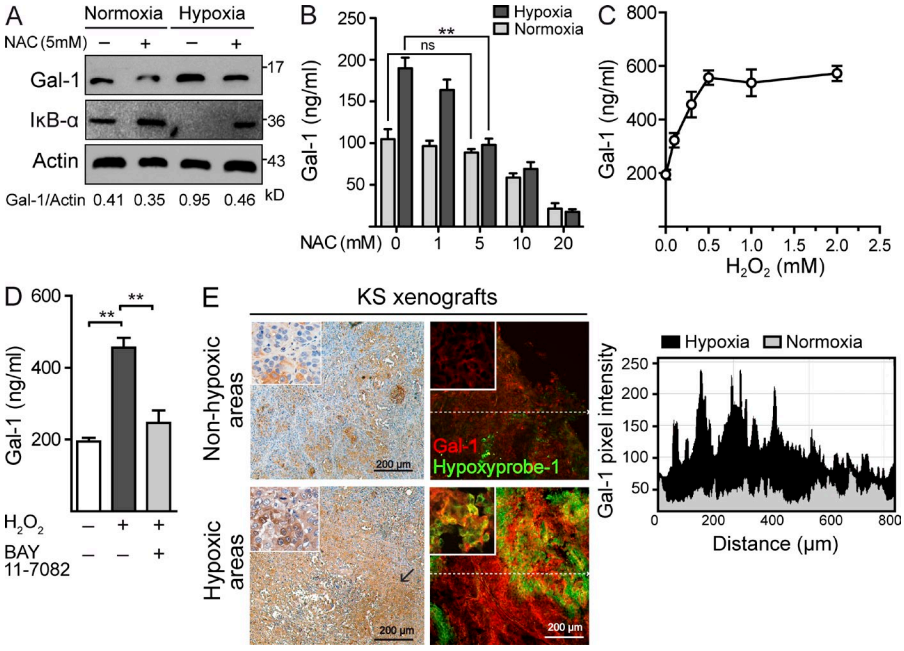

Figure 4. Hypoxia controls Gal-1 expression in KS through mechanisms involving ROS-dependent NF-κB activation. (A) Immunoblot of Gal-1, IκB-α, and actin expression in KS cells cultured under hypoxic or normoxic conditions in the presence or absence of 5 mM of the ROS scavenger NAC. Data are representative of three independent experiments. (B) ELISA of Gal-1 secretion by KS cells cultured under hypoxic or normoxic conditions in the presence of increasing concentrations of NAC. Data are the mean ± SEM of three independent experiments. (C) ELISA of Gal-1 secretion by KS cells cultured with increasing concentrations of H_2O_2. Data are the mean ± SEM of three independent experiments. (D) ELISA of Gal-1 secretion by KS cells exposed to 0.5 mM H_2O_2 in the presence or absence of 1 μM BAY 11–7082. Data are the mean ± SEM of three independent experiments. (E) Immunostaining of Gal-1 and Hypoxyprobe-1 in nonhypoxic and hypoxic areas of KS xenografts. Right, chart shows quantification of pixel intensity of red fluorescence (Gal-1) along the dashed line. Images are representative of three independent experiments. (B and D) **, $P < 0.01$.

As both HIF-dependent and HIF-independent oxygen-sensing mechanisms have been linked to NF-κB–regulated gene transcription (Mizukami et al., 2005; Rius et al., 2008; Fitzpatrick et al., 2011), we next asked whether hypoxia might control Gal-1 expression through NF-κB–regulated pathways. Blockade of NF-κB transcriptional activity by expression of a super-repressor form of the NF-κB inhibitor α (IκB-α-SR) or pharmacological inhibition using BAY-117802 prevented IκB-α degradation and completely eliminated hypoxia-driven Gal-1 expression and secretion without altering the levels of HIF-1α (Fig. 3, A–E and L). Of note, inhibition of NF-κB also suppressed Gal-1 secretion under normoxic conditions (Fig. 3 L), suggesting that this endogenous lectin is a direct transcriptional target of NF-κB. Supporting these observations, analysis of the regulatory sequences of human *LGALS1* gene revealed several putative NF-κB consensus sequences, including a specific site located within the functionally active promoter (Toscano et al., 2011).

As NF-κB activation may result from oxidative stress of hypoxic cells as a result of the generation of ROS (Mizukami et al., 2005), we then examined whether hypoxia may induce NF-κB activation and subsequent up-regulation of Gal-1 through increased production of ROS. Scavenging of ROS using *N*-acetylcysteine (NAC) strongly inhibited induction of Gal-1 expression and secretion and prevented IκB-α degradation in KS cells cultured under hypoxic conditions (Fig. 4, A and B). Moreover, exogenous administration of H_2O_2 stimulated the secretion of Gal-1 in a dose- and NF-κB–dependent fashion (Fig. 4, C and D). These data indicate that ROS-dependent activation of NF-κB may control the induction of proangiogenic Gal-1 in tumor hypoxic microenvironments. Supporting these findings, Gal-1 preferentially localized within hypoxic regions surrounding necrotic areas in the center of KS xenografts injected in vivo into nude mice (Fig. 4 E).

Gal-1–glycan interactions couple tumor hypoxia to pathological angiogenesis in KS

Having defined the molecular pathways underlying hypoxia-regulated Gal-1 expression, we next investigated whether Gal-1–glycan interactions might couple tumor hypoxia to angiogenesis at the tumor-EC interface. To address this question directly, we conducted a series of in vitro and in vivo experiments aimed at disrupting lectin–glycan interactions either by blocking Gal-1 expression or hindering N- or O-glycan elongation. Three different short hairpin RNA (shRNA) constructs targeting unique sequences of Gal-1 (shGal-1.1, shGal-1.2, and shGal-1.3) were stably expressed in KS cells. Retroviral-mediated infection of KS cells with shGal-1.1 or shGal-1.2 suppressed Gal-1 expression and secretion substantially (Fig. 5 A). Serum-free conditioned medium (SFCM) obtained from KS cells exposed to hypoxic conditions induced a considerable increase in the formation of EC tubular networks compared with KS cells incubated under normoxic conditions; this effect was eliminated when Gal-1 was suppressed in KS cells (Fig. 5 B). Additionally, SFCM from KS cells cultured in hypoxic microenvironments augmented angiogenesis when incorporated in vivo into Matrigel plugs. However, hypoxic KS SFCM failed to induce angiogenesis when cells were stably transfected with Gal-1 shRNA (Fig. 5, C and D). This effect proceeded irrespective of whether SFCM from Gal-1 knockdown KS clones were implanted into wild-type (C57BL/6) or Gal-1–deficient (*Lgals1*$^{-/-}$) mice (Fig. 5 C), suggesting that

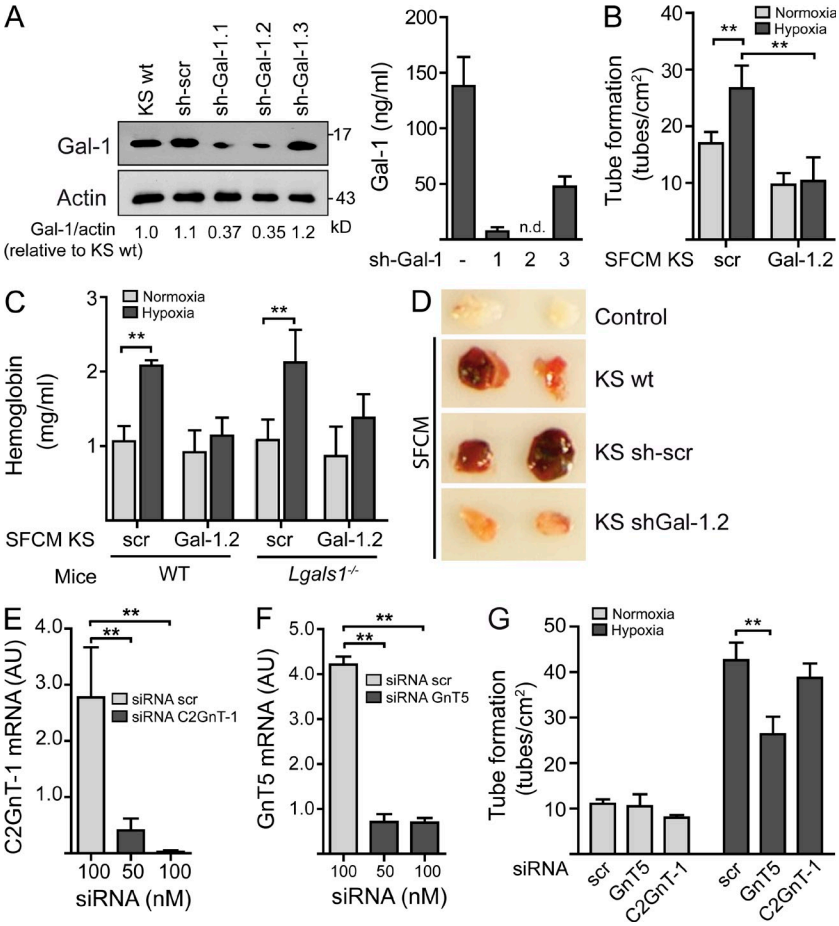

Figure 5. Gal-1–N-glycan interactions link tumor hypoxia to angiogenesis in KS. (A) Immunoblot (left) and ELISA (right) of Gal-1 in KS cells expressing shRNA constructs that target different sequences of human Gal-1 mRNA (sh-Gal-1.1, sh-Gal-1.2 and sh-Gal-1.3) or scrambled shRNA (sh-scr) compared with nontransfected KS cells (KS). Data are representative (left) or are the mean ± SEM (right) of five independent experiments. (B) Tube formation by HUVEC incubated with SFCM from normoxic or hypoxic KS cells transfected or not with scr or Gal-1 shRNA. Data are the mean ± SEM of four independent experiments. (C) Hemoglobin content of Matrigel plugs containing SFCM of KS cells transfected or not with Gal-1 or scr shRNA, cultured under hypoxic or normoxic conditions and inoculated into B6 WT or *Lgals1*$^{-/-}$ mice. Data are the mean ± SEM of three independent experiments. (D) In vivo vascularization of Matrigel plugs containing SFCM of KS cells transfected or not with Gal-1 shRNA or scr shRNA. Data are representative of three independent experiments with three animals per group. (E and F) qRT-PCR analysis of C2GnT-1 (E) or GnT5 (F) mRNA of HUVEC transfected with different concentrations of specific siRNA relative to RN18S1 mRNA (AU: arbitrary units). Data are the mean ± SEM of three independent experiments. (G) Tube formation by HUVEC transfected with GnT5, C2GnT-1, or scr siRNA incubated with SFCM from normoxic or hypoxic KS cells. Data are the mean ± SEM of four independent experiments. (B, C, and E–G) **, $P < 0.01$.

hypoxia-regulated, tumor-derived Gal-1 contributes to angiogenesis independently of the presence or absence of the host endogenous lectin.

Gal-1 recognizes multiple galactose-β1-4-*N*-acetylglucosamine (LacNAc) units, which may be present on the branches of N- or O-linked glycans. Thus, regulated expression of glycosyltransferases during vascular remodeling, which serve to create poly-LacNAc ligands, may determine susceptibility to Gal-1. This includes the *N*-acetylglucosaminyltransferase 5 (GnT5), an enzyme which generates β1,6-*N*-acetylglucosamine–branched complex N-glycans and the core-2 β1-6-*N*-acetylglucosaminyltransferase-1 (C2GnT-1), which elongates core-1 O-glycan structures to generate O-linked poly-LacNAc ligands (Rabinovich and Croci, 2012). To substantiate further the relevance of Gal-1–glycan interactions as bridging partners of hypoxia-driven angiogenesis, we assayed SFCM from hypoxic KS cells with knockdown ECs transfected with GnT5 or C2GnT-1 siRNA (Fig. 5, E and F). Interruption of complex N-glycan branching prevented full induction of tubular networks stimulated by hypoxic KS cells, whereas hampering core-2 O-glycan elongation had no effect (Fig. 5 G), underscoring the critical role of complex N-glycans in coupling hypoxia to tumor angiogenesis.

Because certain cytokines and growth factors induced by KSHV infection act as autocrine or paracrine factors for promoting angiogenesis and driving KSHV oncogenesis (Mesri et al., 2010), we asked whether modulation of Gal-1 expression may influence cytokine release by KS cells. Of note, shRNA-mediated Gal-1 silencing did not affect the secretion of typical KS-derived cytokines, including VEGF, ANGPTL4, and Oncostatin M under hypoxic or normoxic conditions (Fig. 6, A–C). These results suggest that Gal-1 itself may act as a KS-derived factor which, by interacting with EC complex N-glycans, directly connects hypoxia to pathological angiogenesis.

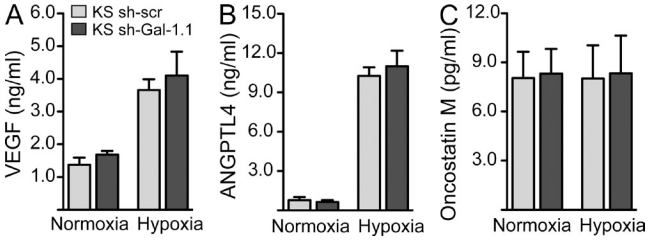

Figure 6. Silencing of Gal-1 expression does not alter the secretion of KS-derived proangiogenic cytokines. (A–C) ELISA of VEGF (A), ANGPTL4 (B), and Oncostatin M (C) secretion by KS cells transfected or not with Gal-1 or scr shRNA and cultured under hypoxic or normoxic conditions. Data are the mean ± SEM of three independent experiments.

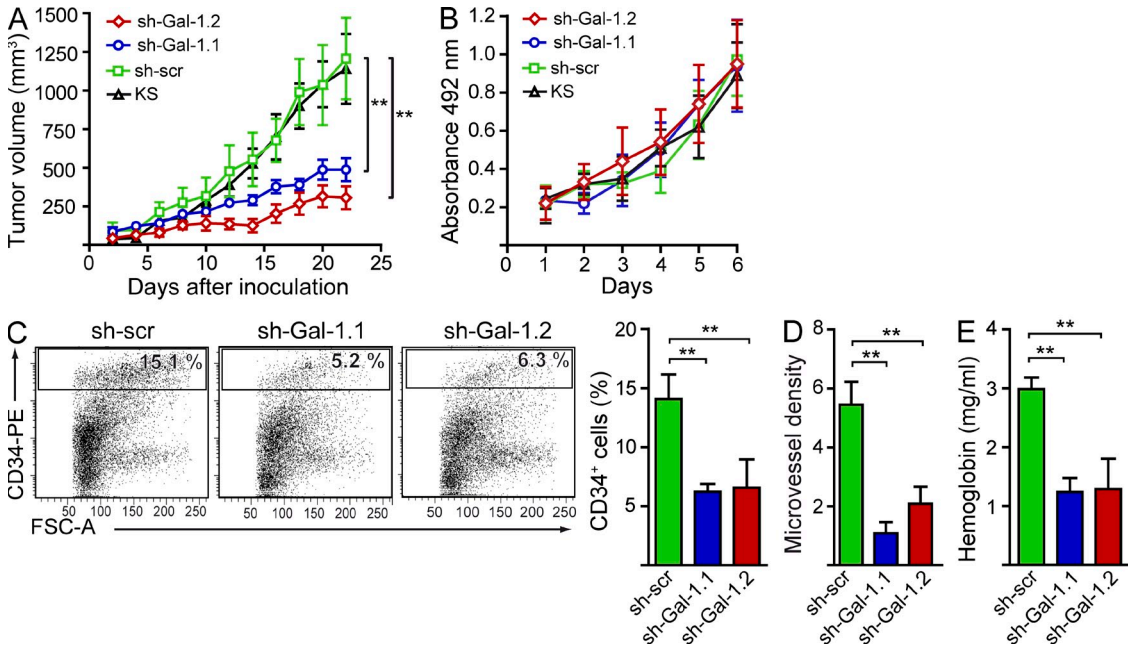

Figure 7. Targeting Gal-1–glycan interactions prevents the angiogenic switch in KS. (A) Tumor growth in nude mice inoculated with 5×10^6 knockdown KS cells expressing Gal-1 shRNA (sh-Gal-1.1 and sh-Gal-1.2), KS cells expressing scr shRNA (sh-scr), or nontransfected KS cells (KS). Data are the mean ± SEM of four independent experiments with five animals per group. (B) In vitro cell growth of KS clones expressing Gal-1 shRNA or scr shRNA (sh-scr) or nontransfected KS cells (KS). Data are the mean ± SEM of three independent experiments. (C) Flow cytometry of tumor-associated $CD34^+$ ECs. Dot plots are representative of four independent experiments. Right, data are the mean ± SEM of four independent experiments. (D) Microvessel density. Data are the mean ± SEM of four independent experiments. (E) Tumor hemoglobin content. Data are the mean ± SEM of four independent experiments. (A and C–E) **, $P < 0.01$.

Targeting Gal-1–glycan interactions prevents the angiogenic switch in KS

To delineate the pathophysiologic relevance of Gal-1–glycan interactions in KS, we first assessed the consequences of Gal-1 inhibition in a xenograft model of human KS in nude mice. Knockdown KS cells expressing Gal-1 shRNA, control KS cells expressing scrambled shRNA (sh-scr), or wild-type KS cells were implanted into the flanks of nude mice. Inoculation of Gal-1 knockdown KS cells led to a considerable reduction in tumor growth (sh-Gal-1.1, 51.2%; sh-Gal-1.2, 60.6% decrease at day 22 after inoculation) compared with mice receiving control KS cells (Fig. 7 A). This effect was not a result of intrinsic differences in proliferation rates, as control KS cells showed no growth advantage in vitro over Gal-1 knockdown cells (Fig. 7 B). Gal-1 silencing attenuated the formation of a typical high density microvessel network as reflected by a substantial decline in the percentage of $CD34^+$ ECs, reduced microvessel density, and considerable reduction of tumor hemoglobin content (Fig. 7, C–E). These results indicate a role for Gal-1–glycan interactions as potential therapeutic targets in KS.

Therapeutic administration of a Gal-1–specific neutralizing mAb promotes tumor regression in established KS

Having established the effects of interrupting the Gal-1–glycan axis in KS, we next evaluated the therapeutic benefit of a recently developed neutralizing Gal-1 mAb, F8.G7 (Ouyang et al., 2011), as a potential agent for the treatment of KS. Given the proangiogenic activity of Gal-1, we first assessed the in vitro effects of F8.G7 mAb in EC biology. Incubation with the Gal-1–specific mAb, but not its isotype control, prevented the binding of Gal-1 to HUVEC at similar levels as lactose, a general galectin inhibitor (Fig. 8 A). The F8.G7 mAb was specific for Gal-1; it did not interfere with the binding of other members of the galectin family, such as Gal-3 or Gal-8, to the EC surface (Fig. 8, B and C), indicating the lack of significant off-target effects. The functional activity of this mAb was demonstrated in vitro through its specific capacity to prevent EC proliferation, migration, invasion, and capillary tube formation induced by Gal-1 (Fig. 8, D–G). Notably, the F8.G7 mAb did not alter EC biology in the absence of exogenous Gal-1 (Fig. 8, E and F).

To validate the therapeutic potential of interrupting Gal-1 signaling in vivo, we infused different doses of the F8.G7 mAb (5 mg/kg, 10 mg/kg, or 50 mg/kg) or the isotype control in nude mice bearing established KS tumors. Treatment of KS-bearing mice with the F8.G7 mAb, but not its isotype control, induced a dose-dependent delay in tumor growth (Fig. 9 A) and suppressed the aberrant vascular network of KS spindle cells, as shown by substantially reduced microvessel density and tumor hemoglobin content (Fig. 9, B and C). To determine whether mAb-mediated Gal-1 blockade affects the in vivo growth and apoptotic rates of tumor cells, we evaluated the extent of 5-ethynyl-2′-deoxyuridine (EdU) incorporation

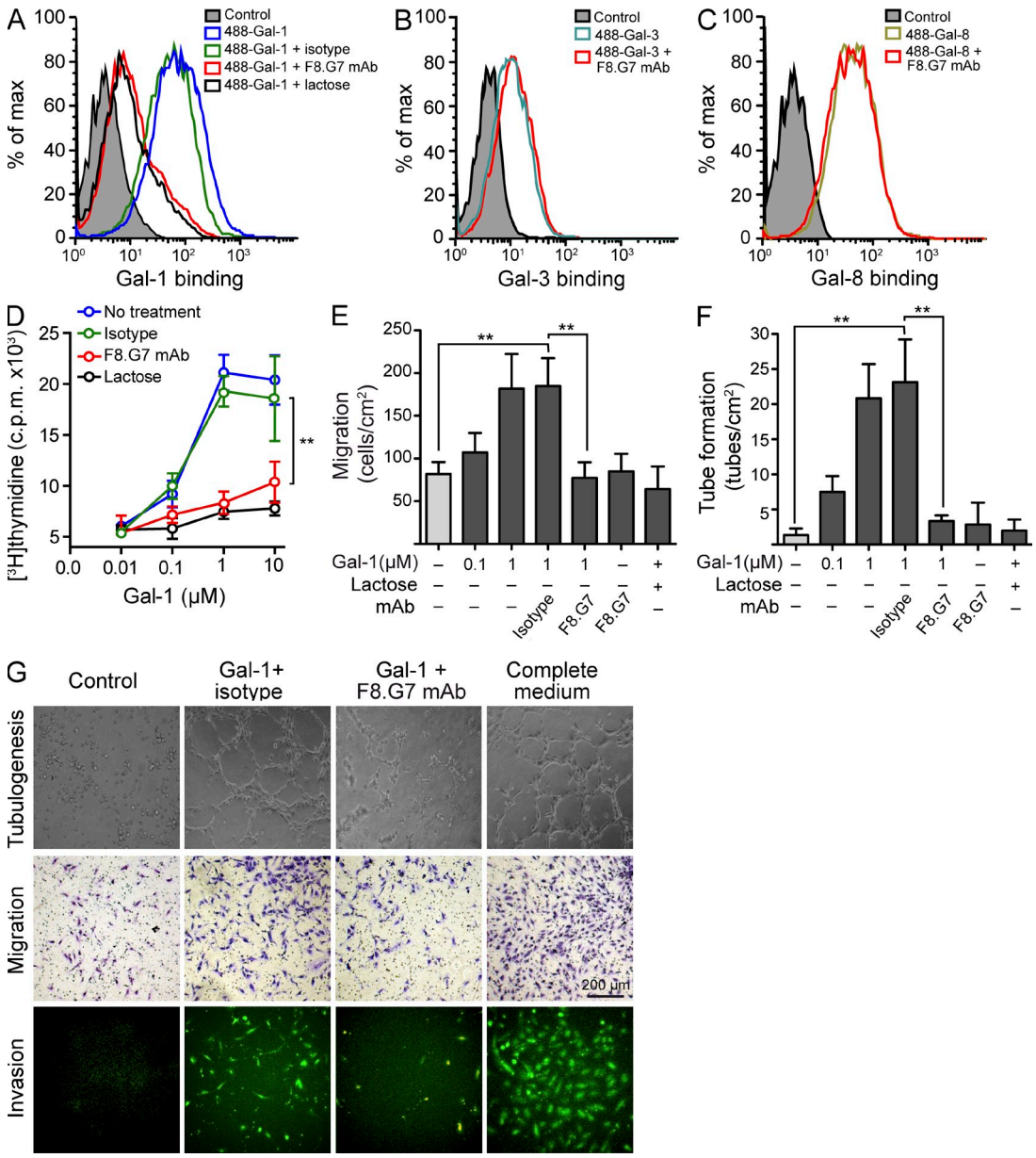

Figure 8. A Gal-1–specific neutralizing mAb prevents Gal-1–induced EC proliferation, migration, invasion, and tube formation. (A) Binding of 20 μg/ml 488-Gal-1 to HUVEC in the presence or absence of 0.5 μM F8.G7 anti-Gal-1 mAb, 0.5 μM isotype control, or 30 mM lactose. Data are representative of three independent experiments. (B and C) Binding of 20 μg/ml 488-Gal-3 (B) or 20 μg/ml 488-Gal-8 (C) to HUVEC in the presence or absence of 0.5 μM F8.G7 anti-Gal-1 mAb. Filled histogram, nonspecific binding determined with unlabeled galectins. Data are representative of three independent experiments. (D–G) Functional activity of F8.G7 mAb in vitro. Proliferation (D), migration (E), and tube formation (F) of HUVEC incubated with or without increasing concentrations of Gal-1 in the presence or absence of 0.5 μM F8.G7 mAb, 0.5 μM isotype control, or 30 mM lactose. (G) Representative micrographs of tube formation (top), migration (middle), and invasion (bottom) of HUVEC exposed to different treatments. Data are the mean ± SEM (D–F) or are representative (G) of three independent experiments. (D–F) **, $P < 0.01$.

and the frequency TUNEL$^+$ cells in tumors isolated from F8.G7 mAb-treated or isotype control mAb-treated mice. Although we observed no differences in the frequency of apoptotic tumor cells (Fig. 9 D, bottom), we found significantly diminished EdU incorporation by KS tumors of mice treated with the anti–Gal-1 F8.G7 mAb compared with mice treated with the isotype control (Fig. 9 D, top), indicating that diminished tumor vascularization induced by Gal-1 blockade was accompanied by reduced tumor growth rates consistent with the common tumor cytostatic effect of anti-angiogenic agents. Of note, injection of the anti–Gal-1 mAb in mice inoculated with Gal-1 knockdown tumor clones had no additional inhibitory effect (not depicted).

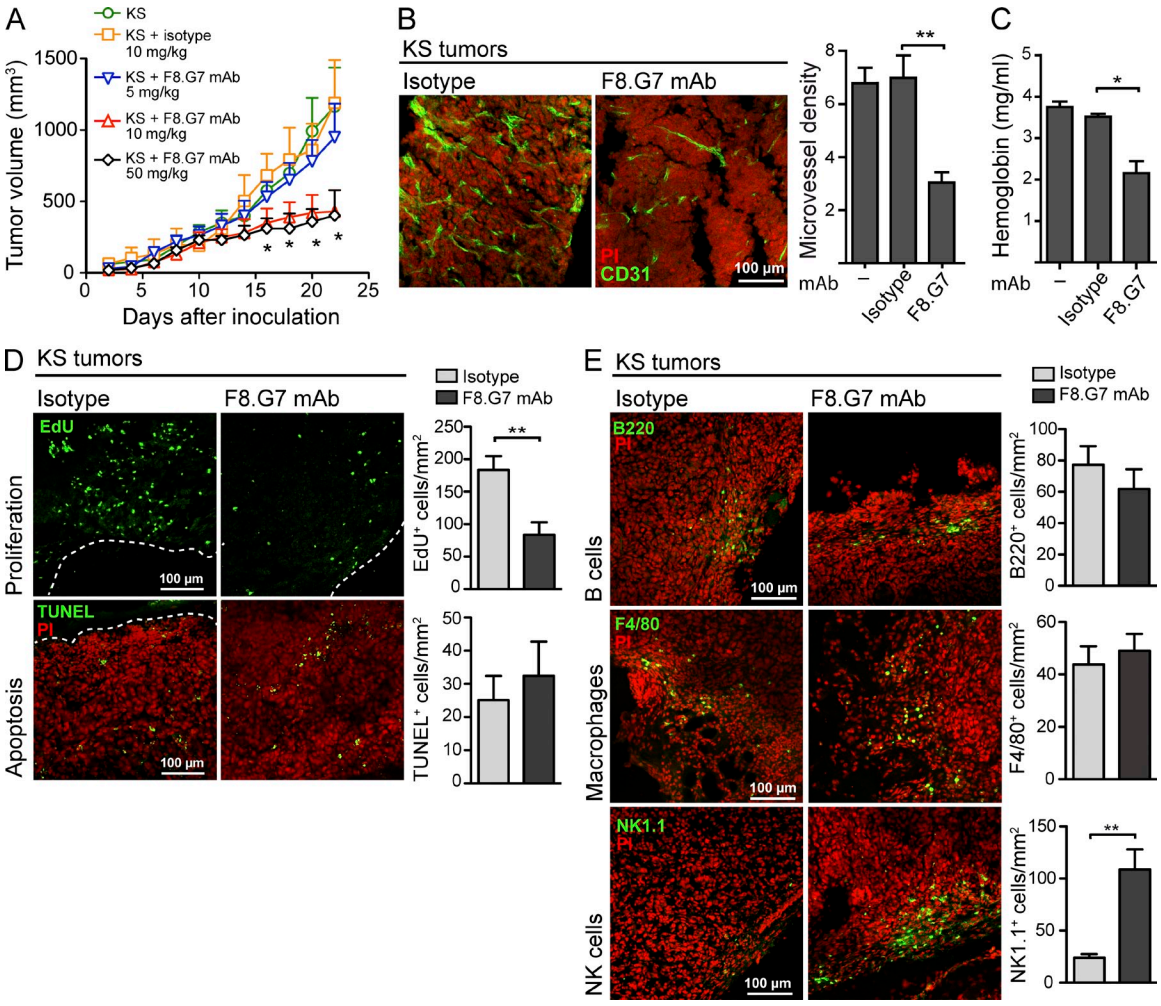

Figure 9. Therapeutic administration of a Gal-1–specific neutralizing mAb promotes tumor regression in established KS. (A–E) Nude mice were inoculated with KS cells and treated in vivo with the indicated doses of F8.G7 mAb or with isotype control when tumors reached 100 mm^3. (A) Kinetics of tumor growth. Data are the mean ± SEM of four independent experiments. (B) Microvessel density. Left, representative confocal micrographs of three experiments are shown (green, CD31; red, propidium iodide). Right, results are the mean ± SEM of three independent experiments. (C) Tumor hemoglobin content. Data are the mean ± SEM of three independent experiments. (D) Top, in vivo proliferation rate of KS xenografts from mice receiving F8.G7 mAb or isotype control, determined by incorporation of EdU injected into mice 2 h before sacrifice. Bottom, apoptosis of tumor sections from mice receiving F8.G7 mAb or isotype control (green, TUNEL; red, propidium iodide). Dashed lines indicate the peripheral borders of the tumor. Data are representative (left) or are the mean ± SEM (right) of three independent experiments. (E) Number of infiltrating B cells ($B220^+$), macrophages ($F4/80^+$), and NK cells ($NK1.1^+$) in tumor sections from mice receiving F8.G7 mAb or isotype control. Data are representative (left) or are the mean ± SEM (right) of three independent experiments with five animals per group. (A–E) *, $P < 0.05$; **, $P < 0.01$.

Given the role of Gal-1 in modulating the interactions between tumors and immune cells (Rabinovich and Croci, 2012), we next evaluated whether Gal-1 blockade in the KS microenvironment resulted in changes in immune cell infiltrates. We found no differences in the frequency of $B220^+$ B cells and $F4/80^+$ macrophages infiltrating KS xenografts from nude mice treated with F8.G7 mAb or isotype control. However, mAb-mediated Gal-1 blockade led to a considerable increase in the number of tumor-infiltrating $NK1.1^+$ NK cells (Fig. 9 E). Thus, therapeutic administration of a Gal-1–specific neutralizing mAb may promote tumor regression in KS through mechanisms involving not only suppression of aberrant angiogenesis but also promotion of NK cell recruitment, expansion, and/or activation.

DISCUSSION

Recent efforts involving genetic manipulation of N- and O-glycosylation pathways, as well as blockade of endogenous galectins, have illuminated essential contributions of lectin–glycan interactions to regulatory circuits that critically influence antitumor responses (Rabinovich and Croci, 2012). In this study, we identified a paracrine circuit, mediated by Gal-1–N-glycan interactions, which connects KSHV infection and tumor hypoxia to the angioproliferative phenotype of KS. Moreover, our findings validate the in vivo therapeutic benefits of a Gal-1–specific mAb capable of promoting tumor regression and counteracting aberrant angiogenesis.

Given its central role in tumor progression, angiogenesis, immunosuppression, and resistance to therapy, tumor hypoxia has been considered one of the best validated targets to be exploited in cancer therapy (Keith et al., 2012). Although much has already been learned about the molecular responses to hypoxia, the highly interactive nature of hypoxia-regulated pathways and the occurrence of tumor-specific divergences in genetic modules regulated by oxygen sensing mechanisms make it difficult to identify the vulnerabilities of hypoxic cells that can be universally exploited as drug targets. Adding complexity to this picture, the molecular mechanisms coupling tumor hypoxia to pathological angiogenesis remain poorly understood. Although HIF-1α and HIF-2α have been proposed as common regulators of hypoxia-driven angiogenesis, emerging evidence supports an essential role for HIF-independent pathways in coupling these processes (Keith et al., 2012). These pathways include the proangiogenic chemokine IL-8, expression of which is regulated by PHD2 (prolyl hydroxylase 2) in an HIF-independent but NF-κB–dependent manner (Mizukami et al., 2005; Chan et al., 2009). Here, we show that ROS-dependent activation of NF-κB in KS tumors controls induction of the endogenous lectin Gal-1, which couples tumor hypoxia to aberrant angiogenesis through direct interactions with N-glycans on the surface of ECs. Although recent studies suggested that Gal-1 is a direct transcriptional target of HIF-1α in colorectal cancer (Zhao et al., 2010), and its expression is controlled by C/EBPα in acute myeloid leukemic cells (Zhao et al., 2011), our findings show that these mechanisms do not operate in the control of KS-derived Gal-1 during hypoxia, suggesting tumor-specific differences in the transcriptional regulation of Gal-1 expression and function. Supporting these observations, we previously identified an activating protein 1 (AP-1)–dependent pathway that controls Gal-1 expression in classical Hodgkin lymphoma (Juszczynski et al., 2007).

Through mechanisms that are still incompletely understood, hypoxia has been reported to be a critical factor in the pathogenesis of KS. Although KSHV infection can increase the transcription of hypoxia-regulated host genes that contribute to the angioproliferative nature of KS, hypoxia may in turn activate KSHV replication and induce the expression of lytic genes (Haque et al., 2003). Accordingly, lytic induction of KSHV and exposure to hypoxic microenvironments can both up-regulate expression of Gal-1 in KS spindle cells. Interestingly, and consistent with a role for this lectin in viral oncogenesis, we previously reported induction of Gal-1 by EBV, another human gammaherpesvirus, through a mechanism driven by the latent membrane proteins LMP2A and LMP1 and mediated by AP-1 and PI3K pathways (Ouyang et al., 2011).

Although our findings demonstrate that ROS-mediated, NF-κB–dependent mechanisms underlie hypoxia-induced Gal-1 expression in KS, the intrinsic roles of ROS and NF-κB in KSHV replication makes it difficult to determine whether these signaling pathways also contribute to KSHV-driven Gal-1 expression. Both latent and lytic KSHV genes, including vFLIP (viral FLICE inhibitory protein), viral G protein–coupled receptor (vGPCR), and K1, have been shown to activate NF-κB and stimulate the secretion of cytokines implicated in KS pathogenesis (Sun et al., 2006; Mesri et al., 2010). Thus, it is tempting to speculate that KSHV gene expression could also control expression of Gal-1 through mechanisms involving NF-κB activation. In addition, recent studies demonstrated that ROS, which can be induced by stress, hypoxia, and inflammation and are implicated in KS tumorigenesis (Ma et al., 2009), can themselves regulate KSHV reactivation and replication, suggesting an alternative pathway of induction of proangiogenic Gal-1 via ROS-dependent KSHV replication (Ye et al., 2011). Supporting these findings, treatment with the ROS inhibitor NAC successfully limited angiogenesis-driven KS progression (Albini et al., 2001) and suppressed KS-like tumors induced by the ROS inducer Rac1 (Ma et al., 2009). Whether these effects involve inhibition of ROS-mediated Gal-1 expression remains to be investigated.

Galectins can modulate EC biology and angiogenesis through different mechanisms. Although Gal-1 directly binds to neuropilin-1 on ECs (Hsieh et al., 2008) and promotes H-Ras signaling to the Raf/ERK (extracellular signal-regulated kinase) kinase cascade (Thijssen et al., 2010), Gal-3 induces EC morphogenesis through binding to N-glycans on $\alpha_v\beta_3$ integrin and modulating surface expression of VEGFR2 (Nangia-Makker et al., 2000; Markowska et al., 2010, 2011). In contrast, Gal-8 triggers EC signaling through binding to the ALCAM (activated leukocyte cell adhesion molecule; CD166; Delgado et al., 2011). As different galectins may be up- or down-regulated in different tumor microenvironments, a detailed galectin signature of different tumors will disclose the best targets for tumor-specific anti-angiogenic therapies. Consistent with its up-regulation in KS gene expression profiles (Cornelissen et al., 2003; Wang et al., 2004), we found that KSHV induces Gal-1 expression which delineates highly angiogenic KSHV LANA$^+$ KS tumors from benign vascular lesions with shared morphological and molecular features, suggesting the potential role of this lectin not only as a therapeutic target but also as a differential diagnostic biomarker. In contrast, a previous study demonstrated that Gal-3 is markedly down-regulated after KSHV replication (Alcendor et al., 2010), suggesting opposing effects of distinct members of the galectin family during KSHV-induced sarcomagenesis. Notably, in our study we show that Gal-1 is up-regulated by both KHSV lytic replication and by hypoxia. This is important because in KS lesions, KSHV$^+$ cells undergoing lytic replication are relatively a minority (Mesri et al., 2010) and thus, this mechanism would not explain why many KS cells of the lesions are indeed Gal-1 positive. Our results showing both KSHV-dependent and -independent mechanisms of Gal-1 induction reveal the contributions of both viral and host factors in its regulation, suggesting the important pathophysiologic role of this endogenous lectin in human KS.

Seeking novel therapeutic approaches, here we validate the in vivo therapeutic benefits of a Gal-1–specific neutralizing mAb capable of inducing tumor regression by attenuating

aberrant angiogenesis. In this regard, galectin inhibitors that block the carbohydrate-recognition domain have been developed for cancer treatment (Ingrassia et al., 2006; Rabinovich et al., 2006; Ito and Ralph, 2012). Although promising, several of these inhibitors lack selectivity for individual members of the galectin family and often display weak ligand affinities. Moreover, anginex, a synthetic peptide which was originally modeled to reproduce the β-sheet structure of anti-angiogenic proteins, efficiently binds to Gal-1 (Thijssen et al., 2006), although it may also recognize other galectins and/or proteins with similar configuration (Salomonsson et al., 2011). These shortcomings can be overcome by a mAb that specifically neutralizes Gal-1 and may target both vascular and immune compartments. Although the T cell compartment could not be investigated here in nude mice, we found that in addition to decreased tumor vascularization, the anti–Gal-1 mAb also enhanced the number of infiltrating NK cells. Whether this effect involves the recruitment, expansion, and/or activation of particular NK cell subsets remains to be elucidated. In this regard, recent studies demonstrated that interactions between Gal-3 and poly-LacNAc–branched core-2 O-glycans decorating tumor-associated MHC I–related chain A (MICA) reduces the affinity of MICA for the activating NK cell receptor NKG2D, thereby impairing NK cell activation and antitumor activity (Tsuboi et al., 2011). Thus, the reduced tumor growth rate observed in mice treated with the anti–Gal-1 mAb could be a result both of reduced vascularization and augmented NK cell–mediated immunity.

Interestingly, given the ability of Gal-1 to eliminate Th1 and Th17 cell subsets selectively (Toscano et al., 2007), and to augment regulatory T (T_{reg}) cell responses (Juszczynski et al., 2007), Gal-1 blockade might also ameliorate AIDS-related KS by restoring the balance between effector and T_{reg} cell populations (Favre et al., 2009). Furthermore, as Gal-1 has been shown to facilitate HIV infection through direct interaction with glycans on viral gp120 and CD4, targeting Gal-1 might also contribute to limit the extent HIV infectivity during disease progression (St-Pierre et al., 2011).

In summary, our findings identify an essential role for Gal-1–N-glycan interactions in connecting KSHV infection and tumor hypoxia to the angioproliferative phenotype of KS and provide novel opportunities for treating KS patients. In addition, our data may have broader implications in other tumors and clinical settings involving deregulated angiogenesis including age-related macular degeneration, diabetes retinopathy, and cardiovascular diseases.

MATERIALS AND METHODS

Mice. *Lgals1*$^{-/-}$ mice (C57BL/6; B6) were provided by F. Poirier (Jacques Monod Institute, Paris, France). Swiss N: NIH(S) nu (nude) mice and C57BL/6 wild-type mice were obtained from the University of La Plata. Mice were bred at the animal facilities of the Institute of Biology and Experimental Medicine according to National Institutes of Health guidelines. All experimental procedures were reviewed and approved by the Institutional Animal Care and Use Committee of the Institute of Biology and Experimental Medicine (IBYME; Buenos Aires, Argentina).

Reagents. Recombinant Gal-1 (rGal-1), rGal-3, and rGal-8 were produced and purified essentially as previously described (Rabinovich et al., 1999; Fernández et al., 2005; Delgado et al., 2011). DyLight 488–conjugated galectins were obtained using DyLight labeling kit (Thermo Fisher Scientific). Inhibitors of NF-κB (BAY 11–7082; 1 μM), ROS (NAC; 5 mM), and lactose (30 mM) were from Sigma-Aldrich. HIF-1α inhibitor (3-(2-(4-Adamantan-1-yl-phenoxy)-acetylamino)-4-hydroxybenzoic acid methyl ester; 3 μM) was from EMD Millipore. Matrigel was from BD. ON-TARGETplus SMART siRNA pools against GnT5, C2GnT-1, HIF-1α, EPAS1 (HIF-2α), C/EBPα, and scrambled (scr) were obtained from Thermo Fisher Scientific. Transfections were performed by Lipofectamine-RNAiMAX (Life Technologies) according to the manufacturer's directions.

Cells and knockdown strategies. KS-Imm is a spontaneously immortalized cell line obtained from a KS biopsy as previously described (Albini et al., 2001). HEK293rKSHV.219 is a KSHV-infected 293 cell line maintained in DME supplemented with 10% FCS as previously described (Vieira and O'Hearn, 2004). The rKSHV219 was provided by J. Vieira (University of Washington, Seattle, WA). iSLK, a KS spindle cell from endothelial lineage infected with rKSHV.219 and a Tet-inducible RTA (Myoung and Ganem, 2011), was provided by D. Ganem (Novartis Institutes for Biomedical Research, Emeryville, CA). Mock-infected and rKSHV.219-infected 293 cells were treated at 70% confluence for 24 h with 3 mM sodium butyrate to induce viral lytic gene expression and replication. rKSHV.219-infected tetracycline-iSLK cells were induced with 0.5 μg/ml doxycycline. All other cell lines were obtained from the American Type Culture Collection. KS, human melanoma (A375), and human prostate carcinoma (LNCaP) cell lines were cultured in RPMI-1640 GlutaMAX complete medium supplemented with 10% FCS. Mouse breast carcinoma (4T1) and mouse melanoma (B16-F0) cell lines were cultured in DME supplemented with 5% FCS (all from Gibco). Primary HUVECs (provided by M. Schattner, Academia Nacional de Medicina, Buenos Aires, Argentina) were maintained in M199 medium supplemented with 20% FCS and 150 μg/ml EC growth supplement (ECGS; BD) and used between passages 2 and 5. Gal-1–specific shRNA was designed and cloned into the pSIREN-RetroQ vector as previously described (Juszczynski et al., 2007). Retroviral shRNA delivery was performed using RetroPack PT-67 packaging cell line (Takara Bio Inc.) according to the manufacturer's instructions. After infection, cells were subjected to puromycin selection (5 μg/ml). The in vitro growth of relevant clones and cells was measured by the MTS assay (Promega).

KS microarrays and data analysis. The Human Genome Array Hg-U133A (Affymetrix) and the Mouse Genome 430 2.0 Array (Affymetrix) were used to examine gene expression profiles in KS biopsies and mECK36 tumors as previously described (Wang et al., 2004; Mutlu et al., 2007). The choice of normal skin as control tissue was the result of an unsupervised clustering of AIDS-KS and several normal tissues. Raw data intensity was analyzed using the GeneSpring 7 (Agilent Technologies) to perform microarray normalization and statistical analysis. The microarray data for mECK36 tumors can be accessed from NCBI's Gene Expression Omnibus (GEO) with accession no. GSE6482, and the microarray data for AIDS-KS can be accessed from European Bioinformatics Institute (EMBL-EBI) with accession no. E-MEXP-66.

Induction of hypoxia. Tumor cell lines were cultured in 24-well plates, placed in a modular incubator chamber (Billups-Rothenberg), and flushed at 2 psi for 10 min with a mixture of 1% O_2, 5% CO_2, and 94% N_2. The chamber was sealed and placed in a 37°C incubator for 18 h. Controls of normoxia were placed in the same incubator at 20% O_2. Chemical induction of HIF-1α was induced after treatment with $CoCl_2$ (Sigma-Aldrich).

Angiogenesis, migration, proliferation, and invasion assays. The formation of capillary-like tubular structures was assessed in Matrigel-coated plates as previously described (Albini et al., 2001). In brief, SFCM from hypoxic or normoxic KS cells infected or not with a retroviral vector containing Gal-1 shRNA was assessed on HUVEC transfected or not with GnT5,

C2GnT-1, or scr siRNA (100 nM). HUVECs (3×10^4 cells/ml) were seeded on Matrigel, incubated at 37°C for periods ranging from 0 to 24 h, and visualized by phase-contrast microscopy. In another set of experiments, HUVECs were exposed to Gal-1 (0.1–3 μM) with or without 30 mM lactose, F8.G7 0.5 μM anti–Gal-1 mAb, or class-matched isotype control Ab (IgG2bλ). Capillary-like tubular structures were scored by counting the number of tubules (closed areas) per cm^2 in a phase-contrast microscope (E-100; Nikon). For migration assays, HUVECs (4×10^4 /well) transfected or not with specific siRNA were resuspended in M199 medium supplemented with 1% FCS. Cells were placed into the top chamber of the insert while the bottom well was filled with rGal-1 in the absence or presence of lactose, F8.G7 mAb, or isotype control or SFCM from KS cells (KS SFCM). After 24 h, inserts were stained with 0.1% crystal violet solution (Sigma-Aldrich) and analyzed in an inverted microscope. For each filter, four images were collected and cells were counted with ImageJ software (1.440; National Institutes of Health). For proliferation assays, HUVECs that were transfected or not with specific siRNA were trypsinized, harvested, and seeded in 96-well microtiter plates (10^3 cells/well). Cells were preincubated for 1 h at 37°C with rGal-1. After 24 h, cells were incubated for an additional 24 h in the presence of 0.8 μCi $[^3H]$-thymidine (NEN Dupont). Cells were then harvested and radioactivity was measured in a 1414 Liquid Scintillation Counter (PerkinElmer). Invasion assays were performed using the BioCoat Angiogenesis System (BD) according to the manufacturer's recommendations. For assessment of in vivo angiogenesis, growth factor–reduced Matrigel (BD) was mixed with SFCM from KS cells infected or not with a retroviral vector expressing Gal-1–specific shRNA and cultured under hypoxic or normoxic conditions. The mixture was then injected subcutaneously into the flanks of either wild-type or *Lgals1*$^{-/-}$ mice or nude mice. Matrigel embedded with buffer alone was used as negative control, and a cocktail containing 50 ng/ml VEGF, 50 U/ml heparin, and 2 ng/ml TNF was used as positive control. After 6 d, Matrigel plugs were collected by surgery, photographed, and weighed. Samples were minced and diluted in water to measure hemoglobin content using the Drabkin reagent kit (Sigma-Aldrich). Each sample was normalized to 100 mg of recovered gel and confronted with a standard curve of mouse blood hemoglobin.

Immunoblotting. Immunoblotting was performed essentially as previously described (Ilarregui et al., 2009). In brief, equal amounts of protein were resolved by SDS-PAGE and blotted onto nitrocellulose membranes (GE Healthcare). After blocking, membranes were probed with rabbit anti–IκB-α 1:500 (C21; Santa Cruz Biotechnology, Inc.), rabbit anti-actin 1:2,000 (I-19; Santa Cruz Biotechnology, Inc.), mouse anti–HIF-1α 1:500 (MA1-516; Thermo Fisher Scientific), mouse anti–HIF-2α 1:500 (NB100122; Novus Biologicals), and rabbit anti-C/EBPα 1:1,000 (2295; Cell Signaling Technology) Abs or 1.5 μg/ml of a rabbit anti–Gal-1 polyclonal IgG obtained and used as previously described (Ilarregui et al., 2009). Blots were then incubated with horseradish peroxidase (HRP)–labeled anti–rabbit or anti–mouse secondary Ab 1:3,000 (Bio-Rad Laboratories) and developed using Immobilon chemiluminescent HRP substrate (Millipore). Protein bands were analyzed with ImageJ.

Real-time quantitative RT-PCR. SYBR green PCR Master Mix was used with ABI PRISM 7500 Sequence Detection Software (all from Applied Biosystems). Primers used were: human Gal-1 forward, 5′-TGAACCTGGGTAAAGACA-3′; and reverse, 5′-TTGGCCTGGTCGAAGGTGAT-3′; human RN18S1 forward, 5′-CGGCCGGGGGCATTCGTATT-3′; and reverse, 5′-TCGCTCTGGTCCGTCTTGCG-3′; human C2GnT-1 forward, 5′-CCTCCTGAGACTCCGGGGTCAGA-3′; and reverse, 5′-CTAGGCGGTCCGTGCCCTAGC-3′; human GnT5 forward, 5′-TGCCCCTGCCGGGACTTCAT-3′; and reverse, 5′-CAGCAGCATGGTGCAGGGCT-3′; human GAPDH forward, 5′-GAGTCAACGGATTTGGTCGT-3′; and reverse: 5′-GACAAGCTTCCCGTTCTCAG-3′; KSHV RTA forward, 5′-CAAGGTGTGCCGTGTAGAGA-3′; and reverse, 5′-TCCCAAAGAGGTACCAGGTG-3′; KSHV GPCR forward, 5′-TGTGTGGTGAGGAGGACAAA-3′; and reverse: 5′-GTTACTGCCAGACCCACGTT-3′; KSHV gB forward, 5′-CTGGGGACTGTCATCCTGTT-3′; and reverse, 5′-ATGCTTCCTCACCAGGTTTG-3′; and KSHV K8.1 forward, 5′-CACCACAGAACTGACCGATG-3′; and reverse, 5′-TGGCACACGGTTACTAGCAC-3′.

Analysis of *LGALS1* promoter constructs with luciferase assay. Cells transfected or not with 100 nM HIF-1α siRNA or 500 ng IκB-α-SR were grown to 60–80% confluence on 24-well plates and cotransfected with 500 ng pGL3-Gal-1-Luc vector containing the *LGALS1* promoter region (−473 to +67) ligated into the pGL3 promoterless reporter vector (Promega) and 20 ng of the control reporter plasmid pRL-TK (Promega) using FUGENE HD transfection reagent (Roche) according to the manufacturer's recommended protocol. After 48 h, culture medium was replaced for RPMI 1% FCS and cells were incubated under normoxic or hypoxic conditions in the absence or presence of NF-κB or HIF-1α inhibitors. After 18 h, cells were lysed and luciferase activity was determined by chemiluminiscence using the dual luciferase assay kit (Promega) in a 20/20^n luminometer (Turner Biosystems). Computational analysis of the *LGALS1* locus (2,400 bp upstream to 2,500 bp downstream to the start site) was performed with the publicly available version of MatInspector software (Genomatix).

ELISA. Soluble Gal-1 was determined using an in-house ELISA. In brief, high binding 96-well microplates (Costar; Corning) were coated with capture Ab (2 μg/ml purified rabbit anti–Gal-1 polyclonal IgG) in 0.1 M sodium carbonate, pH 9.5. After incubation for 18 h at 4°C, wells were rinsed three times with wash buffer (0.05% Tween-20 in PBS) and incubated for 1 h at room temperature with blocking solution (2% BSA in PBS). 100 μl of samples and standards were diluted in 1% BSA and incubated for 18 h at 4°C. Plates were then washed and incubated with 100 ng/ml biotinylated detection Ab (purified rabbit anti–Gal-1 polyclonal IgG) for 1 h. Plates were rinsed three times before adding 0.33 μg/ml HRP-labeled streptavidin (Sigma-Aldrich) for 30 min. After washing, 100 μl TMB solution (0.1 mg/ml tetramethylbenzidine and 0.06% H_2O_2 in citrate-phosphate buffer, pH 5.0) was added to the plates. The reaction was stopped by adding 4N H_2SO_4. Optical densities were determined at 450 nm in a Multiskan MS microplate reader (Thermo Fisher Scientific). A standard curve ranging from 2.5 to 160 ng/ml rGal-1 was run in parallel. Human soluble VEGF (DY293B) and human ANGPTL4 (DY3485) were determined using Duo set ELISA kits (R&D Systems). Oncostatin M was detected using a human ELISA kit (Ab100619; Abcam).

Confocal microscopy, immunohistochemistry, and TUNEL. For immunostaining, mice were anesthetized and cardiac-perfused with PBS and 4% paraformaldehyde, and tissues were embedded in OCT. For confocal microscopy, the following primary Abs were used: rat anti-CD31 (Mec13.3; BD; 1:100), rabbit anti–Gal-1 IgG (1:100), rat anti-LANA (Advanced Biotechnol; 1:1,000), mouse anti-F4/80 (BM8; eBioscience; 1:100), rat anti-B220 (RA3-6B2 BD; 1:100), and rat anti-NK1.1 (PK136; BD; 1:200). Secondary Abs used were anti–rat IgG–Alexa Fluor 488 (Vector Laboratories; 1:500), anti–rat IgG–Texas red (Vector Laboratories; 1:400), anti–rabbit IgG–Alexa Fluor 488 (Cell Signaling Technology; 1:1,000), and anti–rabbit IgG–Alexa Fluor 555 (Cell Signaling Technology; 1:1,000). Hypoxia was detected in vivo after injection of pimonidazole hydrochloride for 30 min after immunostaining with Hypoxyprobe-1 plus kit (Natural Pharmacia). Apoptosis in vivo was determined using an in situ cell death detection kit (TUNEL; Roche) according to the manufacturer's instructions. In vivo proliferation rate was determined using a Click-iT EdU Cell Proliferation Assay (C10337; Life Technologies). In brief, EdU was administered i.p. to mice 2 h before sacrifice. After formalin fixation, EdU was labeled with the Click-iT reaction cocktail according to the manufacturer's instructions. Intestinal sections were used as positive control. For immunoperoxidase, paraffin-embedded human tumor sections were stained with rabbit anti–Gal-1 IgG as previously described (Juszczynski et al., 2007) using the Vectastain Elite ABC kit (Vector Laboratories). These studies were approved by the Institutional Review

Boards of the Hospital de Clínicas "José de San Martín" and the Institute of Biology and Experimental Medicine.

Generation of anti–Gal-1 mAb. The neutralizing anti–Gal-1 (F8.G7) mAb was generated and characterized as previously described (Ouyang et al., 2011).

Binding assays and flow cytometry. ECs were incubated for 1 h at 4°C with DyLight 488–labeled galectins in the absence or presence of lactose, anti–Gal-1 F8.G7 mAb, or isotype control and analyzed on a FACSAria (BD).

In vivo tumor model. 5×10^6 wild-type or knockdown KS cells were injected subcutaneously into 6–8-wk-old nude mice. Treatments with F8.G7 mAb or isotype control (5, 10, or 50 mg/kg; i.p. injections every 3 d) were initiated when tumors reached 100 mm^3. Microvessel density was determined by the number of microvessels present in 10 mm^2. Tumor-associated ECs were identified by flow cytometry using an Alexa Fluor 647–conjugated anti-CD34 antibody (RAM34; eBioscience).

Statistical analysis. Prism software (GraphPad Software) was used for statistical analysis. Two groups were compared with the Student's *t* test for unpaired data. Two-way ANOVA and Dunnett's or Tukey's post-tests were used for multiple comparisons. Nonparametric analysis was performed using a Mann-Whitney *U* test. P-values of 0.05 or less were considered significant.

This work is dedicated to the memory of Mariano Levín (1951–2010).

We thank F. Poirier for *Lgals1*$^{-/-}$ mice, M. Schattner for HUVEC, J. Vieira for rKSHV219, D. Ganem for the iSLK cells, and J. Stupirski, G. Vasen, C. Gatto, and C. Leishman for technical assistance. We also thank H. Rosenberg for critical reading of the manuscript and N. Zwirner for advice.

This work was supported by grants from the Cancer Research Institute (G.A. Rabinovich), Mizutani Foundation for Glycoscience (G.A. Rabinovich), Fundación Sales (G.A. Rabinovich), Agencia Nacional de Promoción Científica y Tecnológica (G.A. Rabinovich; PICT 2010-870), University of Buenos Aires (G.A. Rabinovich), Consejo Nacional de Investigaciones Científicas y Técnicas (M. Salatino and G.A. Rabinovich), the Associazione Italiana per la Ricerca sul Cancro (A. Albini), National Institutes of Health (NIH), National Cancer Institute (NCI; CA136387), and NCI/OHAM supplements to the Developmental Center for AIDS Research (E.A. Mesri; 5P30AI073961), and a Leukemia and Lymphoma Society SCOR grant (M.A. Shipp; #7009-12). We are grateful to Ferioli and Ostry families for generous donations.

We declare no competing financial interests.

Submitted: 9 August 2011
Accepted: 23 August 2012

REFERENCES

Albini, A., M. Morini, F. D'Agostini, N. Ferrari, F. Campelli, G. Arena, D.M. Noonan, C. Pesce, and S. De Flora. 2001. Inhibition of angiogenesis-driven Kaposi's sarcoma tumor growth in nude mice by oral N-acetylcysteine. *Cancer Res.* 61:8171–8178.

Alcendor, D.J., S.M. Knobel, P. Desai, W.Q. Zhu, H.E. Vigil, and G.S. Hayward. 2010. KSHV downregulation of galectin-3 in Kaposi's sarcoma. *Glycobiology*. 20:521–532. http://dx.doi.org/10.1093/glycob/cwp204

Banh, A., J. Zhang, H. Cao, D.M. Bouley, S. Kwok, C. Kong, A.J. Giaccia, A.C. Koong, and Q.T. Le. 2011. Tumor galectin-1 mediates tumor growth and metastasis through regulation of T-cell apoptosis. *Cancer Res.* 71:4423–4431. http://dx.doi.org/10.1158/0008-5472.CAN-10-4157

Casper, C. 2011. The increasing burden of HIV-associated malignancies in resource-limited regions. *Annu. Rev. Med.* 62:157–170. http://dx.doi.org/10.1146/annurev-med-050409-103711

Cedeno-Laurent, F., R. Watanabe, J.E. Teague, T.S. Kupper, R.A. Clark, and C.J. Dimitroff. 2012. Galectin-1 inhibits the viability, proliferation, and Th1 cytokine production of nonmalignant T cells in patients with leukemic cutaneous T-cell lymphoma. *Blood*. 119:3534–3538. http://dx.doi.org/10.1182/blood-2011-12-396457

Cesarman, E., E.A. Mesri, and M.C. Gershengorn. 2000. Viral G protein–coupled receptor and Kaposi's sarcoma: a model of paracrine neoplasia? *J. Exp. Med.* 191:417–422. http://dx.doi.org/10.1084/jem.191.3.417

Chaisuparat, R., J. Hu, B.C. Jham, Z.A. Knight, K.M. Shokat, and S. Montaner. 2008. Dual inhibition of PI3Kalpha and mTOR as an alternative treatment for Kaposi's sarcoma. *Cancer Res.* 68:8361–8368. http://dx.doi.org/10.1158/0008-5472.CAN-08-0878

Chan, D.A., T.L. Kawahara, P.D. Sutphin, H.Y. Chang, J.T. Chi, and A.J. Giaccia. 2009. Tumor vasculature is regulated by PHD2-mediated angiogenesis and bone marrow-derived cell recruitment. *Cancer Cell*. 15:527–538. http://dx.doi.org/10.1016/j.ccr.2009.04.010

Chung, A.S., and N. Ferrara. 2011. Developmental and pathological angiogenesis. *Annu. Rev. Cell Dev. Biol.* 27:563–584. http://dx.doi.org/10.1146/annurev-cellbio-092910-154002

Cornelissen, M., A.C. van der Kuyl, R. van den Burg, F. Zorgdrager, C.J.M. van Noesel, and J. Goudsmit. 2003. Gene expression profile of AIDS-related Kaposi's sarcoma. *BMC Cancer.* 3:7. http://dx.doi.org/10.1186/1471-2407-3-7

Delgado, V.M.C., L.G. Nugnes, L.L. Colombo, M.F. Troncoso, M.M. Fernández, E.L. Malchiodi, I. Frahm, D.O. Croci, D. Compagno, G.A. Rabinovich, et al. 2011. Modulation of endothelial cell migration and angiogenesis: a novel function for the "tandem-repeat" lectin galectin-8. *FASEB J.* 25:242–254. http://dx.doi.org/10.1096/fj.09-144907

Favre, D., S. Lederer, B. Kanwar, Z.M. Ma, S. Proll, Z. Kasakow, J. Mold, L. Swainson, J.D. Barbour, C.R. Baskin, et al. 2009. Critical loss of the balance between Th17 and T regulatory cell populations in pathogenic SIV infection. *PLoS Pathog.* 5:e1000295. http://dx.doi.org/10.1371/journal.ppat.1000295

Fernández, G.C., J.M. Ilarregui, C.J. Rubel, M.A. Toscano, S.A. Gómez, M. Beigier Bompadre, M.A. Isturiz, G.A. Rabinovich, and M.S. Palermo. 2005. Galectin-3 and soluble fibrinogen act in concert to modulate neutrophil activation and survival: involvement of alternative MAPK pathways. *Glycobiology*. 15:519–527. http://dx.doi.org/10.1093/glycob/cwi026

Fitzpatrick, S.F., M.M. Tambuwala, U. Bruning, B. Schaible, C.C. Scholz, A. Byrne, A. O'Connor, W.M. Gallagher, C.R. Lenihan, J.F. Garvey, et al. 2011. An intact canonical NF-κB pathway is required for inflammatory gene expression in response to hypoxia. *J. Immunol.* 186:1091–1096. http://dx.doi.org/10.4049/jimmunol.1002256

Fraisl, P., M. Mazzone, T. Schmidt, and P. Carmeliet. 2009. Regulation of angiogenesis by oxygen and metabolism. *Dev. Cell.* 16:167–179. http://dx.doi.org/10.1016/j.devcel.2009.01.003

Ganem, D. 2010. KSHV and the pathogenesis of Kaposi sarcoma: listening to human biology and medicine. *J. Clin. Invest.* 120:939–949. http://dx.doi.org/10.1172/JCI40567

Haque, M., D.A. Davis, V. Wang, I. Widmer, and R. Yarchoan. 2003. Kaposi's sarcoma-associated herpesvirus (human herpesvirus 8) contains hypoxia response elements: relevance to lytic induction by hypoxia. *J. Virol.* 77:6761–6768. http://dx.doi.org/10.1128/JVI.77.12.6761-6768.2003

Hsieh, S.H., N.W. Ying, M.H. Wu, W.F. Chiang, C.L. Hsu, T.Y. Wong, Y.T. Jin, T.M. Hong, and Y.L. Chen. 2008. Galectin-1, a novel ligand of neuropilin-1, activates VEGFR-2 signaling and modulates the migration of vascular endothelial cells. *Oncogene*. 27:3746–3753. http://dx.doi.org/10.1038/sj.onc.1211029

Ilarregui, J.M., D.O. Croci, G.A. Bianco, M.A. Toscano, M. Salatino, M.E. Vermeulen, J.R. Geffner, and G.A. Rabinovich. 2009. Tolerogenic signals delivered by dendritic cells to T cells through a galectin-1-driven immunoregulatory circuit involving interleukin 27 and interleukin 10. *Nat. Immunol.* 10:981–991. http://dx.doi.org/10.1038/ni.1772

Ingrassia, L., I. Camby, F. Lefranc, V. Mathieu, P. Nshimyumukiza, F. Darro, and R. Kiss. 2006. Anti-galectin compounds as potential anticancer drugs. *Curr. Med. Chem.* 13:3513–3527. http://dx.doi.org/10.2174/092986706779026219

Ito, K., and S.J. Ralph. 2012. Inhibiting galectin-1 reduces murine lung metastasis with increased CD4(+) and CD8 (+) T cells and reduced cancer cell adherence. *Clin. Exp. Metastasis*. 29:561–572. http://dx.doi.org/10.1007/s10585-012-9471-7

Juszczynski, P., J. Ouyang, S. Monti, S.J. Rodig, K. Takeyama, J. Abramson, W. Chen, J.L. Kutok, G.A. Rabinovich, and M.A. Shipp. 2007. The AP1-dependent secretion of galectin-1 by Reed Sternberg cells fosters immune privilege in classical Hodgkin lymphoma. *Proc. Natl. Acad. Sci. USA*. 104:13134–13139. http://dx.doi.org/10.1073/pnas.0706017104

Keith, B., R.S. Johnson, and M.C. Simon. 2012. HIF1α and HIF2α: sibling rivalry in hypoxic tumour growth and progression. *Nat. Rev. Cancer*. 12:9–22.

Kuo, P.L., J.Y. Hung, S.K. Huang, S.H. Chou, D.E. Cheng, Y.J. Jong, C.H. Hung, C.J. Yang, Y.M. Tsai, Y.L. Hsu, and M.S. Huang. 2011. Lung cancer-derived galectin-1 mediates dendritic cell anergy through inhibitor of DNA binding 3/IL-10 signaling pathway. *J. Immunol.* 186: 1521–1530. http://dx.doi.org/10.4049/jimmunol.1002940

Le, Q.T., G. Shi, H. Cao, D.W. Nelson, Y. Wang, E.Y. Chen, S. Zhao, C. Kong, D. Richardson, K.J. O'Byrne, et al. 2005. Galectin-1: a link between tumor hypoxia and tumor immune privilege. *J. Clin. Oncol.* 23:8932–8941. http://dx.doi.org/10.1200/JCO.2005.02.0206

Liu, F.T., and G.A. Rabinovich. 2005. Galectins as modulators of tumour progression. *Nat. Rev. Cancer.* 5:29–41. http://dx.doi.org/10.1038/nrc1527

Ma, Q., L.E. Cavallin, B. Yan, S. Zhu, E.M. Duran, H. Wang, L.P. Hale, C. Dong, E. Cesarman, E.A. Mesri, and P.J. Goldschmidt-Clermont. 2009. Antitumorigenesis of antioxidants in a transgenic Rac1 model of Kaposi's sarcoma. *Proc. Natl. Acad. Sci. USA*. 106:8683–8688. http://dx.doi.org/10.1073/pnas.0812688106

Ma, T., B.C. Jham, J. Hu, E.R. Friedman, J.R. Basile, A. Molinolo, A. Sodhi, and S. Montaner. 2010. Viral G protein-coupled receptor up-regulates Angiopoietin-like 4 promoting angiogenesis and vascular permeability in Kaposi's sarcoma. *Proc. Natl. Acad. Sci. USA*. 107:14363–14368. http://dx.doi.org/10.1073/pnas.1001065107

Markowska, A.I., F.T. Liu, and N. Panjwani. 2010. Galectin-3 is an important mediator of VEGF- and bFGF-mediated angiogenic response. *J. Exp. Med.* 207:1981–1993. http://dx.doi.org/10.1084/jem.20090121

Markowska, A.I., K.C. Jefferies, and N. Panjwani. 2011. Galectin-3 protein modulates cell surface expression and activation of vascular endothelial growth factor receptor 2 in human endothelial cells. *J. Biol. Chem.* 286:29913–29921. http://dx.doi.org/10.1074/jbc.M111.226423

Martin, D., R. Galisteo, Y. Ji, S. Montaner, and J.S. Gutkind. 2008. An NF-kappaB gene expression signature contributes to Kaposi's sarcoma virus vGPCR-induced direct and paracrine neoplasia. *Oncogene*. 27:1844–1852. http://dx.doi.org/10.1038/sj.onc.1210817

Martin, D., R. Galisteo, A.A. Molinolo, R. Wetzker, E. Hirsch, and J.S. Gutkind. 2011. PI3Kγ mediates kaposi's sarcoma-associated herpesvirus vGPCR-induced sarcomagenesis. *Cancer Cell.* 19:805–813. http://dx.doi.org/10.1016/j.ccr.2011.05.005

Mesri, E.A., E. Cesarman, and C. Boshoff. 2010. Kaposi's sarcoma and its associated herpesvirus. *Nat. Rev. Cancer.* 10:707–719. http://dx.doi.org/10.1038/nrc2888

Mizukami, Y., W.S. Jo, E.M. Duerr, M. Gala, J. Li, X. Zhang, M.A. Zimmer, O. Iliopoulos, L.R. Zukerberg, Y. Kohgo, et al. 2005. Induction of interleukin-8 preserves the angiogenic response in HIF-1α-deficient colon cancer cells. *Nat. Med.* 11:992–997.

Montaner, S., A. Sodhi, J.M. Servitja, A.K. Ramsdell, A. Barac, E.T. Sawai, and J.S. Gutkind. 2004. The small GTPase Rac1 links the Kaposi sarcoma-associated herpesvirus vGPCR to cytokine secretion and paracrine neoplasia. *Blood.* 104:2903–2911. http://dx.doi.org/10.1182/blood-2003-12-4436

Montaner, S., A. Sodhi, A.K. Ramsdell, D. Martin, J. Hu, E.T. Sawai, and J.S. Gutkind. 2006. The Kaposi's sarcoma-associated herpesvirus G protein-coupled receptor as a therapeutic target for the treatment of Kaposi's sarcoma. *Cancer Res.* 66:168–174. http://dx.doi.org/10.1158/0008-5472.CAN-05-1026

Mutlu, A.D., L.E. Cavallin, L. Vincent, C. Chiozzini, P. Eroles, E.M. Duran, Z. Asgari, A.T. Hooper, K.M. La Perle, C. Hilsher, et al. 2007. *In vivo*-restricted and reversible malignancy induced by human herpesvirus-8 KSHV: a cell and animal model of virally induced Kaposi's sarcoma. *Cancer Cell.* 11:245–258. http://dx.doi.org/10.1016/j.ccr.2007.01.015

Myoung, J., and D. Ganem. 2011. Generation of a doxycycline-inducible KSHV producer cell line of endothelial origin: maintenance of tight latency with efficient reactivation upon induction. *J. Virol. Methods.* 174:12–21. http://dx.doi.org/10.1016/j.jviromet.2011.03.012

Nangia-Makker, P., Y. Honjo, R. Sarvis, S. Akahani, V. Hogan, K.J. Pienta, and A. Raz. 2000. Galectin-3 induces endothelial cell morphogenesis and angiogenesis. *Am. J. Pathol.* 156:899–909. http://dx.doi.org/10.1016/S0002-9440(10)64959-0

Norling, L.V., A.L. Sampaio, D. Cooper, and M. Perretti. 2008. Inhibitory control of endothelial galectin-1 on in vitro and in vivo lymphocyte trafficking. *FASEB J.* 22:682–690. http://dx.doi.org/10.1096/fj.07-9268com

Ouyang, J., P. Juszczynski, S.J. Rodig, M.R. Green, E. O'Donnell, T. Currie, M. Armant, K. Takeyama, S. Monti, G.A. Rabinovich, et al. 2011. Viral induction and targeted inhibition of galectin-1 in EBV+ posttransplant lymphoproliferative disorders. *Blood*. 117:4315–4322. http://dx.doi.org/10.1182/blood-2010-11-320481

Paulson, J.C., O. Blixt, and B.E. Collins. 2006. Sweet spots in functional glycomics. *Nat. Chem. Biol.* 2:238–248. http://dx.doi.org/10.1038/nchembio785

Paz, A., R. Haklai, G. Elad-Sfadia, E. Ballan, and Y. Kloog. 2001. Galectin-1 binds oncogenic H-Ras to mediate Ras membrane anchorage and cell transformation. *Oncogene*. 20:7486–7493. http://dx.doi.org/10.1038/sj.onc.1204950

Rabinovich, G.A., and D.O. Croci. 2012. Regulatory circuits mediated by lectin-glycan interactions in autoimmunity and cancer. *Immunity*. 36: 322–335. http://dx.doi.org/10.1016/j.immuni.2012.03.004

Rabinovich, G.A., G. Daly, H. Dreja, H. Tailor, C.M. Riera, J. Hirabayashi, and Y. Chernajovsky. 1999. Recombinant galectin-1 and its genetic delivery suppress collagen-induced arthritis via T cell apoptosis. *J. Exp. Med.* 190:385–398. http://dx.doi.org/10.1084/jem.190.3.385

Rabinovich, G.A., A. Cumashi, G.A. Bianco, D. Ciavardelli, I. Iurisci, M. D'Egidio, E. Piccolo, N. Tinari, N. Nifantiev, and S. Iacobelli. 2006. Synthetic lactulose amines: novel class of anticancer agents that induce tumor-cell apoptosis and inhibit galectin-mediated homotypic cell aggregation and endothelial cell morphogenesis. *Glycobiology*. 16:210–220. http://dx.doi.org/10.1093/glycob/cwj056

Rius, J., M. Guma, C. Schachtrup, K. Akassoglou, A.S. Zinkernagel, V. Nizet, R.S. Johnson, G.G. Haddad, and M. Karin. 2008. NF-kappaB links innate immunity to the hypoxic response through transcriptional regulation of HIF-1α. *Nature.* 453:807–811. http://dx.doi.org/10.1038/nature06905

Rubinstein, N., M. Alvarez, N.W. Zwirner, M.A. Toscano, J.M. Ilarregui, A. Bravo, J. Mordoh, L. Fainboim, O.L. Podhajcer, and G.A. Rabinovich. 2004. Targeted inhibition of galectin-1 gene expression in tumor cells results in heightened T cell-mediated rejection; A potential mechanism of tumor-immune privilege. *Cancer Cell.* 5:241–251. http://dx.doi.org/10.1016/S1535-6108(04)00024-8

Salomonsson, E., V.L. Thijssen, A.W. Griffioen, U.J. Nilsson, and H. Leffler. 2011. The anti-angiogenic peptide anginex greatly enhances galectin-1 binding affinity for glycoproteins. *J. Biol. Chem.* 286:13801–13804. http://dx.doi.org/10.1074/jbc.C111.229096

St-Pierre, C., H. Manya, M. Ouellet, G.F. Clark, T. Endo, M.J. Tremblay, and S. Sato. 2011. Host-soluble galectin-1 promotes HIV-1 replication through a direct interaction with glycans of viral gp120 and host CD4. *J. Virol.* 85:11742–11751. http://dx.doi.org/10.1128/JVI.05351-11

Sun, Q., H. Matta, G. Lu, and P.M. Chaudhary. 2006. Induction of IL-8 expression by human herpesvirus 8 encoded vFLIP K13 via NF-kappaB activation. *Oncogene*. 25:2717–2726. http://dx.doi.org/10.1038/sj.onc.1209298

Tang, D., Z. Yuan, X. Xue, Z. Lu, Y. Zhang, H. Wang, M. Chen, Y. An, J. Wei, Y. Zhu, et al. 2012. High expression of Galectin-1 in pancreatic stellate cells plays a role in the development and maintenance of an immunosuppressive microenvironment in pancreatic cancer. *Int. J. Cancer.* 130:2337–2348. http://dx.doi.org/10.1002/ijc.26290

Thijssen, V.L., R. Postel, R.J. Brandwijk, R.P. Dings, I. Nesmelova, S. Satijn, N. Verhofstad, Y. Nakabeppu, L.G. Baum, J. Bakkers, et al. 2006. Galectin-1 is essential in tumor angiogenesis and is a target for antiangiogenesis therapy. *Proc. Natl. Acad. Sci. USA*. 103:15975–15980. http://dx.doi.org/10.1073/pnas.0603883103

Thijssen, V.L., B. Barkan, H. Shoji, I.M. Aries, V. Mathieu, L. Deltour, T.M. Hackeng, R. Kiss, Y. Kloog, F. Poirier, and A.W. Griffioen. 2010. Tumor cells secrete galectin-1 to enhance endothelial cell activity.

Cancer Res. 70:6216–6224. http://dx.doi.org/10.1158/0008-5472.CAN-09-4150

Toscano, M.A., G.A. Bianco, J.M. Ilarregui, D.O. Croci, J. Correale, J.D. Hernandez, N.W. Zwirner, F. Poirier, E.M. Riley, L.G. Baum, and G.A. Rabinovich. 2007. Differential glycosylation of TH1, TH2 and TH-17 effector cells selectively regulates susceptibility to cell death. *Nat. Immunol.* 8:825–834. http://dx.doi.org/10.1038/ni1482

Toscano, M.A., L. Campagna, L.L. Molinero, J.P. Cerliani, D.O. Croci, J.M. Ilarregui, M.B. Fuertes, I.M. Nojek, J.P. Fededa, N.W. Zwirner, et al. 2011. Nuclear factor (NF)-κB controls expression of the immunoregulatory glycan-binding protein galectin-1. *Mol. Immunol.* 48:1940–1949. http://dx.doi.org/10.1016/j.molimm.2011.05.021

Tsuboi, S., M. Sutoh, S. Hatakeyama, N. Hiraoka, T. Habuchi, Y. Horikawa, Y. Hashimoto, T. Yoneyama, K. Mori, T. Koie, et al. 2011. A novel strategy for evasion of NK cell immunity by tumours expressing core2 O-glycans. *EMBO J.* 30:3173–3185. http://dx.doi.org/10.1038/emboj.2011.215

Vieira, J., and P.M. O'Hearn. 2004. Use of the red fluorescent protein as a marker of Kaposi's sarcoma-associated herpesvirus lytic gene expression. *Virology.* 325:225–240. http://dx.doi.org/10.1016/j.virol.2004.03.049

Wang, H.W., M.W. Trotter, D. Lagos, D. Bourboulia, S. Henderson, T. Mäkinen, S. Elliman, A.M. Flanagan, K. Alitalo, and C. Boshoff. 2004. Kaposi sarcoma herpesvirus-induced cellular reprogramming contributes to the lymphatic endothelial gene expression in Kaposi sarcoma. *Nat. Genet.* 36:687–693. http://dx.doi.org/10.1038/ng1384

Wu, F.Y., Q.Q. Tang, H. Chen, C. ApRhys, C. Farrell, J. Chen, M. Fujimuro, M.D. Lane, and G.S. Hayward. 2002. Lytic replication-associated protein (RAP) encoded by Kaposi sarcoma-associated herpesvirus causes p21CIP-1-mediated G1 cell cycle arrest through CCAAT/enhancer-binding protein-α. *Proc. Natl. Acad. Sci. USA.* 99:10683–10688. http://dx.doi.org/10.1073/pnas.162352299

Ye, F., F. Zhou, R.G. Bedolla, T. Jones, X. Lei, T. Kang, M. Guadalupe, and S.J. Gao. 2011. Reactive oxygen species hydrogen peroxide mediates Kaposi's sarcoma-associated herpesvirus reactivation from latency. *PLoS Pathog.* 7:e1002054. http://dx.doi.org/10.1371/journal.ppat.1002054

Zhao, X.Y., T.T. Chen, L. Xia, M. Guo, Y. Xu, F. Yue, Y. Jiang, G.Q. Chen, and K.W. Zhao. 2010. Hypoxia inducible factor-1 mediates expression of galectin-1: the potential role in migration/invasion of colorectal cancer cells. *Carcinogenesis.* 31:1367–1375. http://dx.doi.org/10.1093/carcin/bgq116

Zhao, X.Y., K.W. Zhao, Y. Jiang, M. Zhao, and G.Q. Chen. 2011. Synergistic induction of galectin-1 by CCAAT/enhancer binding protein α and hypoxia-inducible factor 1α and its role in differentiation of acute myeloid leukemic cells. *J. Biol. Chem.* 286:36808–36819. http://dx.doi.org/10.1074/jbc.M111.247262